Representing Spatial Information for Limb Movement: Role of Area 5 in the Monkey

F. Lacquaniti,[1,2] E. Guigon,[2] L. Bianchi,[2] S. Ferraina,[3] and R. Caminiti[3]

[1]Istituto di Fisiologia umana, Università di Cagliari, Cagliari, [2]INB-CNR, Istituto Scientifico S. Lucia, Rome, and [3]Istituto di Fisiologia umana, Università La Sapienza, Rome, Italy

How is spatial information for limb movement encoded in the brain? Computational and psychophysical studies suggest that beginning hand position, via-points, and target are specified relative to the body to afford a comparison between the sensory (e.g., kinesthetic) reafferences and the commands that generate limb movement. Here we propose that the superior parietal lobule (Brodmann area 5) might represent a substrate for a body-centered positional code. Monkeys made arm movements in different parts of 3D space in a reaction-time task. We found that the activity of area 5 neurons can be related to either the starting point, or the final point, or combinations of the two. Neural activity is monotonically tuned in a body-centered frame of reference, whose coordinates define the azimuth, elevation, and distance of the hand. Each spatial coordinate tends to be encoded in a different subpopulation of neurons. This parcellation could be a neural correlate of the psychophysical observation that these spatial parameters are processed in parallel and largely independent of each other in man.

What is computed in reaching a target and where in the brain? A vector code of movement direction has been described in primary motor cortex M1 (Georgopoulos et al., 1982; Schwartz et al., 1988; Caminiti et al., 1990), dorsal premotor cortex PMd (Caminiti et al., 1991; Fu et al., 1993), areas 2 and 5 of the parietal cortex (Kalaska et al., 1983; Cohen et al., 1994), and cerebellum (Fortier et al., 1989). Many neurons at all these sites are broadly tuned to the direction of the hand movement. Preferred directions (PDs) tend to be distributed uniformly throughout space, and the population vector predicts well the hand trajectory (Georgopoulos et al., 1988).

A vector code of movement direction implies that neural activity should be the same for the same movement performed along parallel directions but starting from different initial positions. It has been found, however, that this is not the case for many neurons in M1 (Caminiti et al., 1990) and PMd (Caminiti et al., 1991). The PDs computed in each part of the workspace rotate by an amount and direction that are highly variable among cells. Taken at face value, the results of this analysis would lead to the conclusion that, because the tuning parameters of neurons appear to change across workspace, the representation of limb movement is fragmented in many local subregions centered at each different starting position of the hand (Caminiti et al., 1990, 1991; Burnod et al., 1992).

An alternative view, however, is that locations of the hand and target are encoded in a fixed reference frame for movements performed in different parts of the workspace. If so, one should be able to characterize neural activity by means of just one set of tuning parameters that apply globally to different parts of the workspace, independently of initial hand position or target location. Psychophysical studies have indicated that in the process of transforming sensory information about target and hand position into motor commands, reaching movements are specified in a body-centered frame of reference (Soechting and Flanders, 1989a; Jeannerod, 1991; Paillard, 1991).

The present view reconciles the neural code during movement with the code during maintenance of static posture. It is well known that static cell discharge is monotonically related to the corresponding position of the hand in space in M1 (Georgopoulos et al., 1984; Georgopoulos and Massey, 1985; Kettner et al., 1988), PMd (Caminiti et al., 1991), area 2 (Soechting et al., 1992), and area 5 (Georgopoulos et al., 1984; Georgopoulos and Massey, 1985).

We have searched evidence for coherent representations of movement and posture in the dorsal part of parietal area 5 of the monkey (see Mountcastle et al., 1975). This is essentially a somatosensory and somatomotor center, endowed with a wide representation of the arm. Most neurons have pure somesthetic receptive fields that are generally larger than those found in area 2 (Duffy and Burchfiel, 1971; Burbaud et al., 1991). These fields are often multimodal (extero- and proprioceptive) and receive inputs from one or more limb segments (Duffy and Burchfiel, 1971; Sakata et al., 1973; Mountcastle et al., 1975; Burbaud et al., 1991). Single joint neurons reflect sensitively steady joint positions (Mountcastle et al., 1975). There is another population of neurons whose discharge is modulated weakly by passive mobilization of the limb but strongly by active movements (Mountcastle et al., 1975; Kalaska et al., 1983; Burbaud et al., 1991).

When the activities of area 5 neurons are analyzed according to the scheme of vector coding of movement direction, they appear to be directionally tuned in the same manner as the neurons of M1 and PMd (Kalaska et al., 1983, 1990; Ferraina and Bianchi, 1994). The prevalence of static positional effects is higher in area 5 than in frontal areas (Georgopoulos et al., 1984). An important functional difference between frontal and parietal cortex emerges when static loads pulling the arm in different directions are applied to the monkey's arm during planar arm movements (Kalaska et al., 1989, 1990). Load sensitivity forms a relative continuum in M1; some neurons are very sensitive to the applied load and appear to encode parameters related to movement dynamics (forces and torques), whereas other neurons are relatively insensitive to loads and appear to encode movement kinematics, and still other neurons fall in between, exhibiting both directional and load tuning (Kalaska et al., 1990). By contrast, the vast majority of neurons in area 5 are essentially insensitive to loads; they appear to encode only movement kinematics, not dynamics (Kalaska et al., 1990).

In the present study tuning properties of area 5 neurons have been analyzed according to two different schemes: (1) vector code of movement direction and (2) positional code in body-centered coordinates.

Materials and Methods

General Procedures

General methodological procedures were the same as in previous studies (Caminiti et al., 1990, 1991; Ferraina and Bianchi, 1994). Head-fixed monkeys (*Macaca nemestrina*) sat on a primate chair in front of the apparatus (Fig. 1*a*,*b*). The targets consisted of 1-cm-diameter transparent push buttons that could be retroilluminated. Sixteen of

Cerebral Cortex Sep/Oct 1995;5:391–409; 1047-3211/95/$4.00

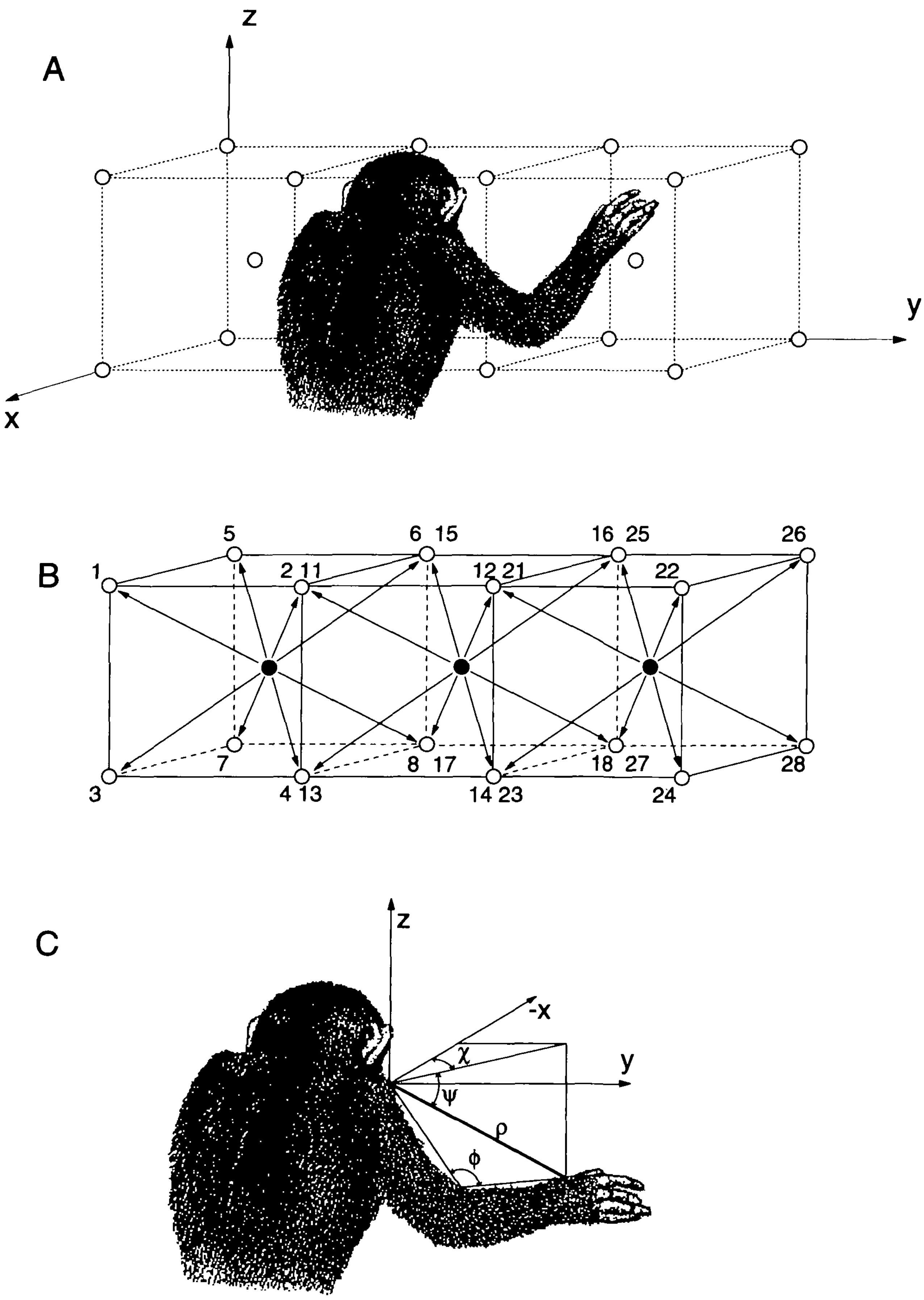
A
z
y
x
B
5
6 15
16 25
26
1
2 11
12 21
22
7
8 17
18 27
28
3
4 13
14 23
24
C
z
-x
y
χ
ψ
ρ
ϕ

the buttons were placed at the vertices of three horizontally adjoined, imaginary cubes. Three other buttons were placed at the centers of the cubes. Cubes had 10-cm-long sides, 8.7 cm center-to-vertex distance. The center of the central cube was in the midsagittal plane at shoulder height, 25 cm in front of the animal. Monkeys were trained to perform in a reaction-time task. A trial began with the illumination of the center button in a given cube. The monkey was required to push it for the duration of a control time (1.5-2.5 sec), until the center light was turned off and one of the targets at the vertices of the same cube was turned on. Within specified upper limits of reaction time (0.35 sec) and movement time (1 sec), the monkey was required to move the hand toward the target button and push it for a variable duration (1-1.5 sec). A liquid reward was delivered and a new trial was started after a random intertrial interval (1-1.5 sec). Targets were presented in pseudo-random order until five movements were performed correctly to each of the eight vertices of that cube. The same sequence was then repeated for the two other cubes.

The location of selected points on the monkey was measured ultrasonically (GP-8-3D, Science Accessories Corp.). To this end small emitters were attached to the head, and to the limb at the shoulder, elbow and wrist joints. Four microphones mounted on the wall picked up the ultrasonic signals and the x,y,z-coordinates of each emitter relative to a laboratory-fixed frame (Fig. 1*a*) were calculated after conversion of signal transmission time to distance. Spatial resolution was ≈0.1 mm.

Electrical activity of cortical neurons was recorded extracellularly using standard techniques (Caminiti et al., 1990) from the dorsal area 5 contralateral to the performing arm. Data from the right hemisphere and left arm were mirror transformed. At the end, the animals were sacrificed with an overdose of Nembutal and computer-assisted histological procedures were used to locate the electrode tracks (Caminiti et al., 1990).

Data Analysis

Each trial was divided as follows: (1) center-holding time (CT), the last 1 sec before the presentation of the target; (2) reaction time (RT), from the target presentation to the release of the center button; (3) movement time (MT), from the release of the center button to the depression of the target button; (4) target-holding time (THT), the last 0.5 sec during which the target button remained pressed before the reward was given. RMT was the interval from 200 msec before to 200 msec after movement onset. Mean parameters related to both limb geometry and neural activity were computed by averaging over different epochs for each cell and each trial.

Limb Geometry

The position of the wrist was defined using a number of alternative coordinate systems.

Cartesian: anteroposterior (x), mediolateral (y), and vertical (z) coordinates. Posterior, lateral, and upward directions were taken to be positive. This frame of reference was parallel to the setup (see Fig. 1*a*).

Spherical: elevation angle (ψ) relative to the horizontal (positive upward), azimuth angle (χ) relative to the sagittal (positive rightward), and radial distance (ρ) from the origin. Two different origins were used: the midpoint between the eyes, and the shoulder joint (Soechting and Flanders, 1989a). The latter case is illustrated in Figure 1*c*.

Spherangular: a hybrid coordinate system centered at the shoulder, defined by two parameters of the spherical coordinate system (elevation and azimuth angles) and by the angle of extension at the elbow (ϕ, Fig. 1*c*). ϕ is related to the radial distance ρ of the wrist from the shoulder by $\phi = \cos^{-1}[(l_1^2 + l_2^2 - \rho^2)/2l_1l_2]$, where l_1 and l_2 are the length of the upper arm and forearm, respectively, with typical values of 13 cm. Note that the spherangular coordinate system differs from the spherical system because it is dimensionally homogeneous (all spatial parameters in angular units).

Orientation Angles. These are the four angles that give the absolute orientation of the upper arm and forearm (Soechting and Flanders, 1989b). Elevations (θ, β) are the angles between the upper arm or the forearm and the vertical axis. They are measured in the vertical plane. Yaws (η, α) are the angles between the upper arm or the forearm and the anterior direction. They are measured in the horizontal plane.

All derived coordinates were computed trigonometrically from the measured Cartesian coordinates (Soechting and Flanders, 1989a,b). Mean initial positions in specified coordinates were computed by averaging over CT, and mean final positions were computed over THT. In the following, $\mathbf{q}_i$ and $\mathbf{q}_f$ denote the vectors of initial positions and final positions, respectively.

To determine the extent to which arm posture varied among different trials with the same target, each orientation angle was regressed on a cubic polynomial in shoulder-centered spherical coordinates of the wrist. Multivariate regressions were performed using standard least-squares techniques (Morrison, 1990):

$$\mathbf{w}_f = U(\mathbf{p}_f) \qquad (1)$$

$\mathbf{w}_f$ denotes the vector of orientation angles (θ, β, η, α), whereas $\mathbf{p}_f$ denotes the vector of wrist position in spherical coordinates (ψ, χ, ρ). $U()$ is a polynomial linear in the coefficients, and including first-, second-, and third-degree position terms. The multiple regression was performed over the ensemble of data (5 repetitions × 24 targets × 131 cells, $n = 15{,}720$).

Analysis of Neural Activity

Positional Properties. Neural activity during stationary posture at the targets was related to final wrist position according to a polynomial model:

$$r(\mathrm{THT}) = V(\mathbf{q}_f) \qquad (2)$$

$r(\mathrm{THT})$ is the mean firing rate over THT. $V()$ is a polynomial linear in the coefficients, and of first, second, or third degree in the position terms, depending on the model. $\mathbf{q}_f$ was expressed in Cartesian, spherical, spherangular, or angular coordinates, depending on the coordinate system chosen to describe limb position. All targets ($n = 24$) and repetitions ($n = 5$) were used in the regressions for each cell. Statistical significance of the regression model was assessed by means of an F test ($\alpha = 0.05$). In addition to the complete regression model, partial models were also assessed by means of standard iterative procedures (Morrison, 1990). Essentially, one term at a time was removed from the complete best-fitting model and the residual variance of the resulting partial model was tested against that of the complete model (F test, $\alpha = 0.05$; see also Fu et al., 1993). The total correlation coefficients of the models were computed for all cells with significant regressions, and their Z-transformed values were averaged across these cells to yield a mean R.

To test whether the firing rate during center-holding time, $r(\mathrm{CT})$, was explained by the same regression model that explained $r(\mathrm{THT})$, the values of initial positions ($\mathbf{q}_i$) were used in Equation 2 to predict $r(\mathrm{CT})$. Predicted and actual activities were then statistically compared.

Mean firing rate during movement time, $r(\mathrm{MT})$, was fitted by means of a linear combination of initial positions and of the difference between the final and initial positions:

$$r(\mathrm{MT}) = M(\mathbf{q}_i) + N(\mathbf{q}_f - \mathbf{q}_i), \qquad (3)$$

where $M()$ and $N()$ are polynomials of first degree. $M = 0$ implies that the cell's discharge is correlated with the variational terms only. $N = 0$ implies that the cell's discharge is correlated with initial position. $M = N$ implies that the cell's discharge is correlated with final position. Finally, when $M \neq N \neq 0$, the cell's discharge depends on both the initial position term and the variational term. Inequality tests were based on >10% differences between terms and statistical difference ($\alpha = 0.05$) from zero. To determine the relative contribution of initial position, final position, and difference between the two, a further model was assessed that included a linear combination of

←

Figure 1. *a*, Experimental apparatus. *Open circles* indicate the targets; *x*, *y*, *z*, the laboratory-fixed Cartesian axes. *b*, Layout of the workspace. Movements of constant amplitude were required from one of three possible starting points (*solid circles*) in one of eight possible directions (*arrows*). Targets denoted by *pairs of numbers* (e.g., *2 11*) could be reached from two different starting points. *c*, Shoulder-centered reference frame. Wrist coordinates are elevation ψ, azimuth χ, and distance ρ. *a* and *b* are modified from Caminiti et al. (1991).

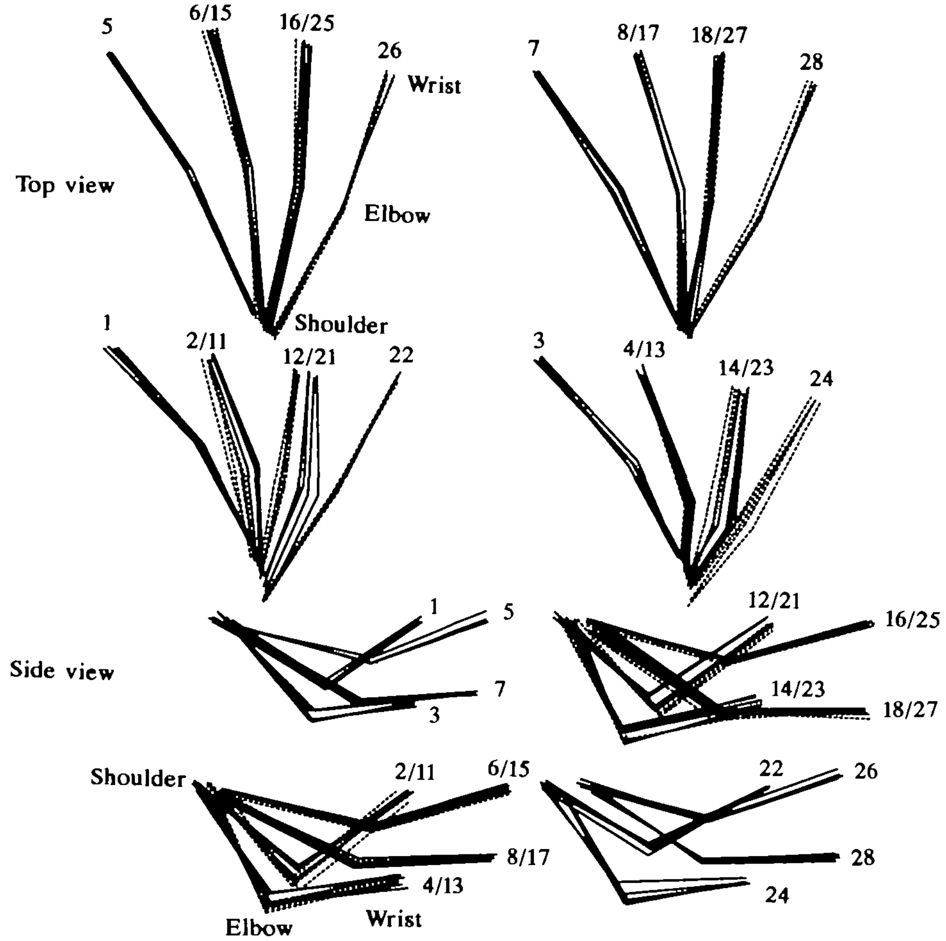

Figure 2. Stick diagrams of limb geometry at the targets. All trials ($n = 5$) for one cell recording have been superimposed, in *continuous lines* for odd-numbered targets and in *dashed lines* for even-numbered targets. Targets are numbered as in Figure 1*b*. *Top four panels*, arm projections on a horizontal plane seen from above the monkey; *bottom four panels*, arm projections on a sagittal plane.

these three terms (the right member of Eq. 3 included also that of Eq. 2). Partial models were then constructed by removing the terms that did not explain significant portions of the total variance (see above).

Clearly, the model of Equation 3 can account for both positional and directional properties. However, we assumed that whatever set of tuning parameters characterizes a given neuron, it applies to all three parts of the experimental workspace. Accordingly, Equation 3 (as Eq. 2) was fitted simultaneously to the ensemble of the data obtained for all 24 targets. The constraint of fixed tuning parameters was absent instead in the directional analysis described in the next section.

Directional Properties in Each Cube Separately. This analysis followed the procedures previously described (Georgopoulos et al., 1982, 1988; Schwartz et al., 1988; Caminiti et al., 1990, 1991). Briefly, the mean firing rate during either RT, MT, or RMT was linearly regressed on the Cartesian components of all movement directions ($n = 8$) in each cube separately. Movement direction is a vector of unit length pointing from initial to final position. Statistical significance of the regression was assessed by means of an F test ($\alpha = 0.05$). The vector of PD was then computed from the coefficients of the linear regression for each directionally tuned neuron and in each cube separately.

Directional tuning during movement was compared with positional tuning during stationary posture in the following manner. The static positional gradient **G** of each cell was determined from the multiple linear regression of THT activity and the Cartesian coordinates of the hand at all targets (Kettner et al., 1988). **G** is a unit length vector in the direction of the maximum change in neuronal discharge related to target positions. The orientation of **G** was then compared with that of the corresponding PDs by computing their inner product in each cube separately. Because both **G** and PD were taken as unit length vectors, their inner product corresponds to the cosine of the angle between these vectors.

Results

Behavior

For each movement the distance between center and peripheral targets was constant. Accordingly, movements were performed under roughly comparable conditions in all parts of the workspace. On average, the RT was 266 ± 10 msec (mean ± SE) over the eight targets of the left cube, 261 ± 6 msec in the center cube, and 261 ± 11 msec in the right cube. MT was 618 ± 39 msec in the left cube, 574 ± 32 msec in the center cube, and 611 ± 41 msec in the right cube. Intertrial variability was not negligible, however; on average ($n = 24$), the SD over five movements to the same target was 44 and 149 msec for RT and MT, respectively.

Figure 2 shows the geometrical configurations of the arm corresponding to the final positions at all targets (numbered as in Fig. 1*b*). All trials ($n = 5$) for one cell recording have been superimposed, in continuous lines for odd-numbered targets and in dashed lines for even-numbered targets.

The reaching workspace of the monkey was tested over a wide portion of the anatomical range. In the shoulder-centered spherical frame, the azimuth angle of the wrist ranged from about −55° to 45°, elevation from −40° to 15°, and distance from 10 to 35 cm. In spherangular coordinates, elbow extension ranged from 50° to 160°. In angular coordinates, upper arm yaw ranged from −45° to 90°, upper arm elevation from 5° to 80°, forearm yaw from −70° to 35°, and forearm elevation from 90° to 145°. Though limited, there was some variation of the center of rotation of the shoulder joint. This depended on a shoulder translation associated with move-

Table 1

Regression of joint angles versus wrist position

Joint angle	R_M	R_L	Distance	Azimuth	Elevation
Upper arm yaw	0.925	0.906	−0.025	0.956	−0.462
Upper arm elevation	0.963	0.962	0.031	0.040	0.916
Forearm yaw	0.979	0.974	0.004	1.011	−0.045
Forearm elevation	0.941	0.931	−0.019	−0.004	0.944

Each orientation angle (θ, β, η, α) was regressed on the spherical coordinates (distance, azimuth, elevation) of wrist position over the ensemble of data (5 repetitions × 24 targets × 131 cells, n = 15,720). Data are, from left to right, multiple correlation coefficients (R_M) for the cubic regression, those (R_L) for the linear regression, and the coefficients of the linear terms.

ments directed to distant targets. The SDs of its Cartesian coordinates relative to a laboratory-fixed frame were about 1 cm (<10% of upper arm length).

An important question regarding arm posture in this task is whether or not there exists motor equivalence for movements directed to a given target (Lacquaniti and Maioli, 1994). In a redundant limb, such as the monkey arm, a given 3D position of the wrist can be obtained by means of several different combinations of angular values at the shoulder and elbow joints. To address this problem, we computed the SD of the Cartesian coordinates of the final position of either the wrist or the elbow over five movements to the same target. A mean SD for each such coordinate was then obtained over all targets and neurons (24 × 131, n = 3144). The values were the following: x, 1.80 ± 1.27 mm (mean ± SD) at the wrist and 1.84 ± 1.80 mm at the elbow; y, 2.26 ± 1.18 mm and 2.87 ± 1.55 mm, respectively; z, 2.03 ± 1.07 mm and 2.64 ± 1.44 mm, respectively. Thus, mean SDs were quite small, those of elbow coordinates being only slightly greater than the corresponding ones of wrist coordinates. This indicates that the postures associated with any given target were highly stereotypical, presumably because the monkeys were overtrained in the task.

The lack of motor equivalence implies that the specific geometric configuration of the limb (joint angles) is completely determined by the endpoint (wrist) position only. In other words, the values of joint angles covary tightly with the values of wrist position. To demonstrate this point directly, each angular coordinate (orientation angles, θ, β, η, α) was linearly regressed on the three spherical coordinates of wrist position (Eq. 1). Regression parameters are shown in Table 1. It can be noted that the correlation coefficients are high (R > 0.9) in all cases, even with the simple linear model. As

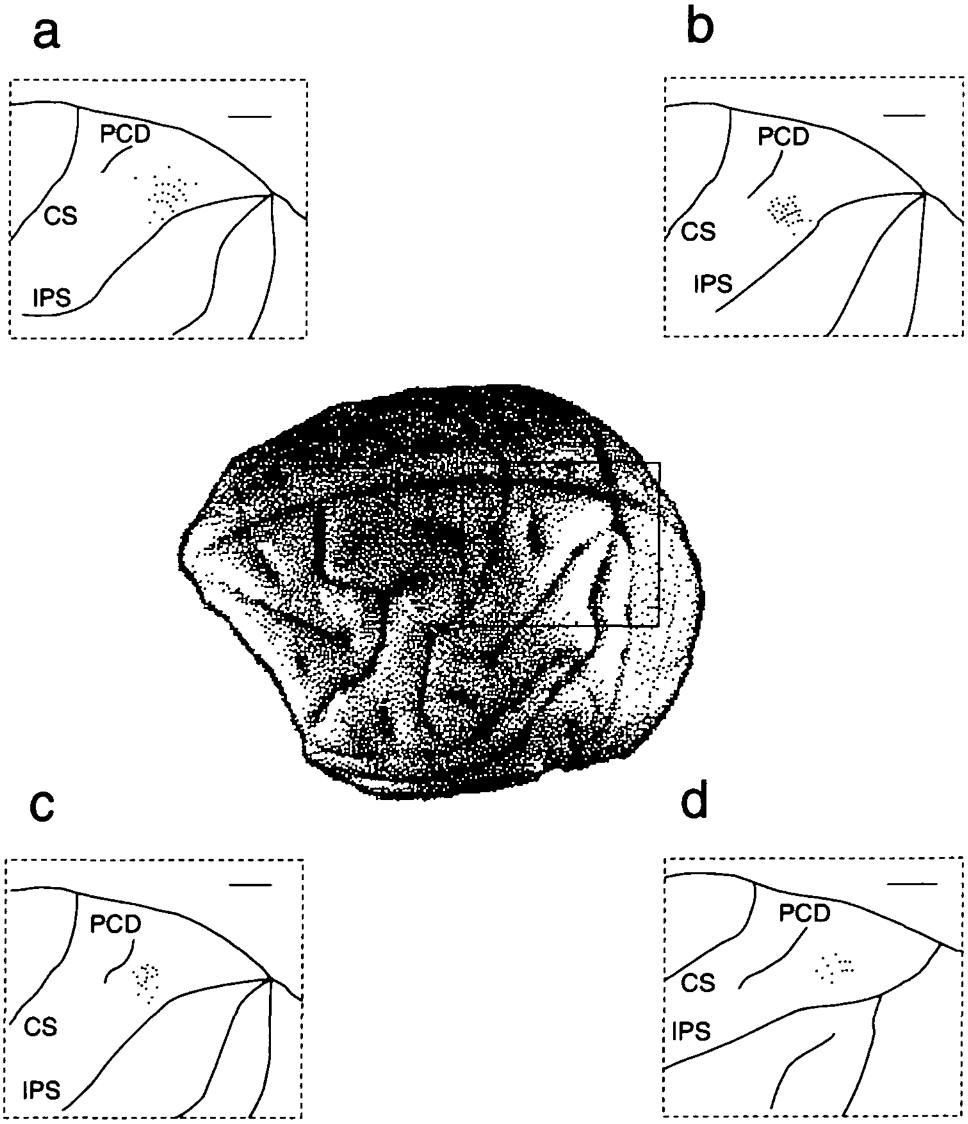

Figure 3. Microelectrode penetrations in dorsal area 5. *a–d* are enlargements of the region outlined in the *brain figurine*. *Dots* indicate entry points of penetrations. In one animal penetrations were made in the left hemisphere but are shown in a mirror-reversed right hemisphere (*b*) to facilitate the comparison with data obtained in the other animals. *IPS*, *CS*, intraparietal and central sulci, respectively; *PCD*, postcentral dimple. Scale bars, 0.5 cm.

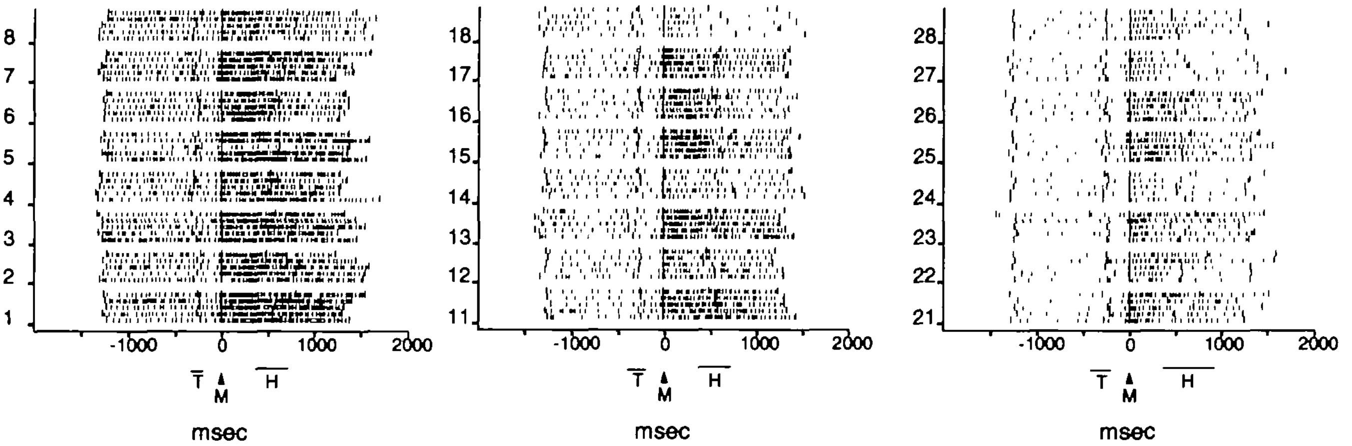

Figure 4. Impulse activity of a neuron with movements to different targets. Rasters of five replications for each target in the *left, center, and right cubes* are aligned with the movement onset (*M*). Target presentation is indicated by *T*; beginning of target-holding time, by *H*. *Longer vertical bars* indicate, *from left to right*, beginning of the trial, target presentation, movement onset, and beginning and end of target-holding time. *Numbers on the vertical axes* correspond with the targets of Figure 1*b*.

expected, yaw angles are related mostly to wrist azimuth, whereas elevation angles depend on both wrist elevation and distance (Soechting and Flanders, 1989b).

Neurophysiological Data Base

Two hundred nine arm-related neurons were recorded during 74 successful microelectrode penetrations in four hemispheres of three monkeys from the dorsal area 5 contralateral to the performing arm. Electrode penetration tracks were located in a cortical region that is caudal to the postcentral dimple and spans most of the exposed part of area 5 up to the crown of the dorsal bank of the intraparietal sulcus (Fig. 3). All cells recorded in dorsal area 5 fired during active movements and most of them (80%) responded also to passive joint rotations and/or manipulations of deep tissues of the upper arm and forearm. One hundred thirty-one neurons of the total sample had a complete set of experimental repetitions for all targets and were retained for further quantitative analysis.

Figure 4 shows in raster form the variations in activity of one neuron for all movements. It can be noted that the discharge changes in an orderly manner with the changes in target location, during both movement and posture. Thus, the activity is highest for target 1 and lowest for target 24, which is at the opposite extreme of the workspace (see Fig. 1*b*). In the following we describe first the postural activity of the neurons and then their movement activity.

Activity of Area 5 Neurons during Stationary Posture

In agreement with previous 2D studies of area 5 (Georgopoulos et al., 1984; Georgopoulos and Massey, 1985), we found that the mean activity of most neurons reflects accurately the position of the wrist in space during the maintenance of stationary posture at both center and peripheral targets. The relationship between the changes in the mean neural activity at the targets and the corresponding changes in the position of the wrist is illustrated for six neurons in Figure 5. Wire frames correspond to the three workspaces depicted in the insets, offset horizontally for clarity. The wire-frame corners indicate the position of the wrist relative to the shoulder at the end of the movement to the corresponding target. Wrist position has been averaged over THT across all trials ($n = 5$) to each target. Wire frames are substantially distorted relative to the cubes defined by the corresponding targets, because the final position of the wrist was not constant relative to the target for movements directed to different targets. In particular, targets at the extremes of the workspace (e.g., targets 5 and 26) were reached with the fingers more extended than targets closer to the monkey; the distance between wrist and target was then correspondingly greater (see also Fig. 2). These spatial anisotropies were reflected in the neural discharge.

The neurons plotted in Figure 5 demonstrate in a paradigmatic manner the general features of the vast majority of area 5 neurons. Their mean activity (gray bars at wire-frame corners) was related quasi-monotonically to the changes in wrist position through all points of the tested workspace. Each neuron was tuned best to the changes of only one out of the three spatial coordinates of the wrist. Thus, the mean discharge of neurons *A* and *B* was related to the azimuth of the wrist relative to the body, increasing from right to left in *A* and from left to right in *B*. The activity of neurons *C* and *D*, instead, was strongly modulated by the distance of the wrist from the body: the closer the wrist, the greater the neural activity in *C*, and the smaller the activity in *D*. Finally, the activity of neurons *E* and *F* was related to wrist elevation, increasing in the downward direction in *E* and in the upward direction in *F*. It must be noted that, although the neurons were best tuned along one coordinate axis, they were not totally selective. For instance, the activity of neuron *B* increased not only with increasing azimuth, but also with decreasing elevation. The issue of the degree of selectivity will be addressed in a following section.

A simple linear model of final wrist position (spherical coordinates relative to the shoulder) predicts the actual discharge of these neurons reasonably well throughout the workspace. This can be appreciated by comparing the gray bars (data) with the corresponding black bars (model) in Figure 5; 64% of the neurons were fitted by this model, with a mean *R* of 0.739. Figure 6 shows the frequency distribution of the regression parameters over the ensemble of neurons. All spatial coefficients (including the intercept) are distributed over a wide range, centered around zero.

We assessed a number of alternative models and the results are summarized in Table 2. On average the differences in the goodness of fit were small among the linear models, independent of the coordinate system used to describe the position of the wrist in space. This is due to the fact that the monkey performed the reaching movements with head fixed and with limited motion of the torso. Moreover, wrist position covaried tightly with the angular coordinates at the shoulder and elbow joints (see Behavior, above). Thus, neurons that were related to wrist azimuth were also related to its y-coordinate in

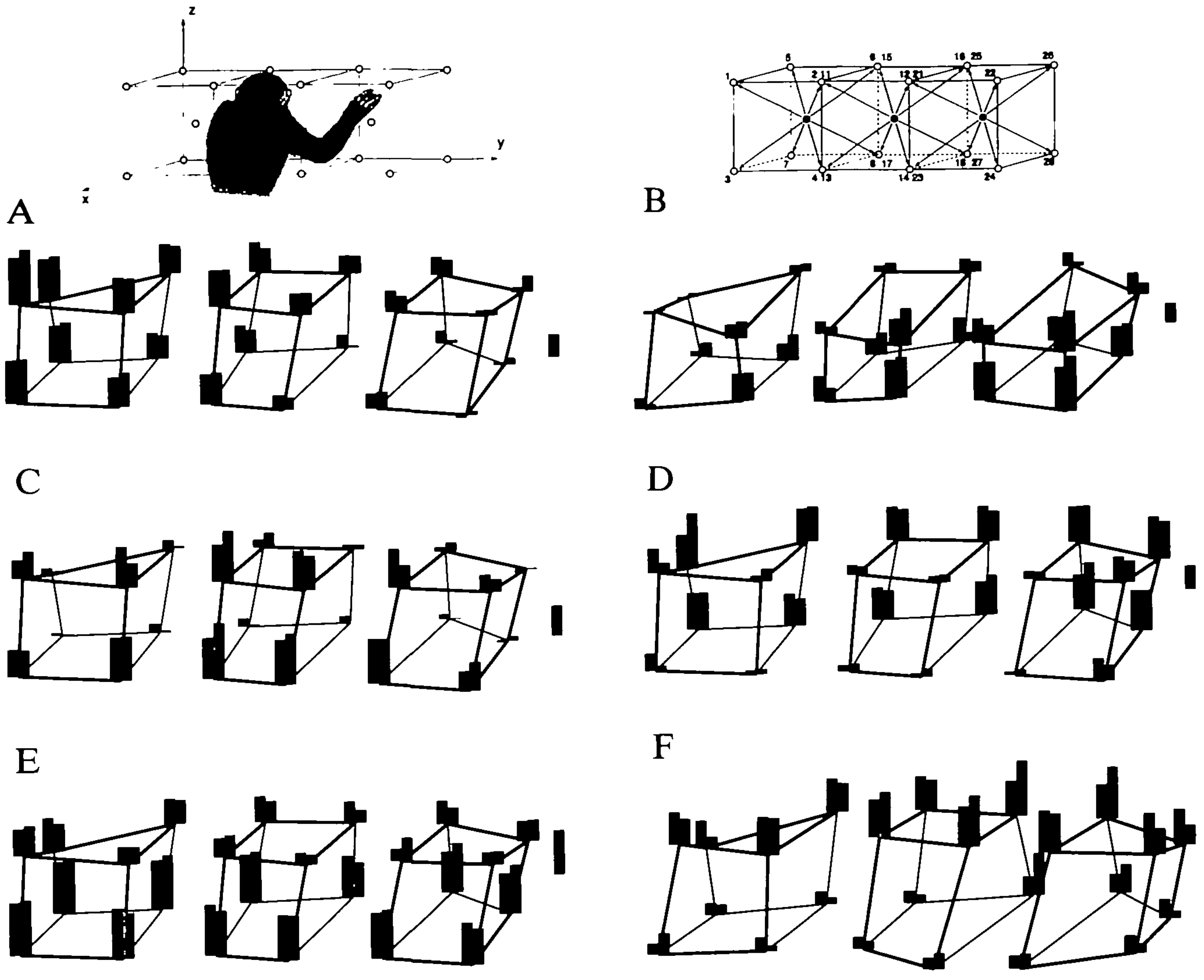

Figure 5. Mean activity of six neurons during static posture at the targets. *Wire frames* correspond to the three workspaces depicted in the *insets*, offset horizontally for clarity. Plots are in parallel projection to preserve the scale. *Wire-frame corners* indicate the position of the wrist relative to the shoulder at the end of the movement to the corresponding target. *Gray bars* adjacent to each corner indicate the firing rate averaged during THT. *Black bars* indicate the firing rate predicted by a linear model of final wrist position in shoulder-centered spherical coordinates. Wrist position and firing rate have been averaged across all trials ($n = 5$) to each target. The multiple correlation coefficients (R), and the coefficients of the position terms from the partial model are, for *A*, (0.827), -4.29χ; *B*, (0.738), $-0.12\rho + 2.63\chi - 4.96\psi$; *C*, (0.818), -0.33ρ; *D*, (0.778), 0.35ρ; *E*, (0.873), $-1.23\chi - 6.70\psi$; *F*, (0.525), 8.95ψ. Calibration bars (to the *right* of each panel), 20 spikes/sec.

the Cartesian frame, and with the yaw angles in the angular coordinate system; similar covariations were observed for the other corresponding coordinates. On average, however, body-centered coordinate systems (spherical, spherangular, and angular) provided a better account of neural modulation (higher correlation coefficients in Table 2) as compared with a Cartesian coordinate system parallel to the laboratory frame. We shall take up this issue in a subsequent section.

Models involving either quadratic or cubic functions of the final position fitted the data much worse than the linear model, because they predicted nonmonotonic changes of activity with limb position. However, higher-order models including both the quadratic and the cubic positional terms, in addition to the linear ones, fitted the data better than the linear model (see Table 2). This is because higher-order terms allowed to follow local nonlinearities. The magnitude of these local deviations from linearity was generally small (<20%) compared to the linear slope. However, local nonlinearities were substantial in the responses of some neurons. For instance, they are appreciable in the case of the neuron *F* in Figure 5 for targets 16, 25, 18, and 27. In this cell the *R* of the linear model (corresponding to the black bars in Fig. 5) was 0.525, whereas the *R* of the nonlinear model (linear + quadratic + cubic terms) was 0.908.

Neural activity during CT at starting locations was generally related to initial wrist position by the same regression coefficients that accounted for the THT activity at the targets. CT discharge predicted by this regression did not differ significantly from recorded CT discharge in 81% of the neurons.

Segregation of Different Spatial Coordinates in Distinct Subpopulations of Neurons

Inspection of the data in the format of Figure 5 revealed that the modulation of neural activity was often related selectively to just one of three spatial coordinates, and that the preferred coordinate varied among neurons. We followed standard statistical procedures (Morrison, 1990) to assess quantitatively the contribution of each spatial parameter to the net discharge of each neuron. Eigenvectors were computed from the covariance matrix associated with the multivariate regression

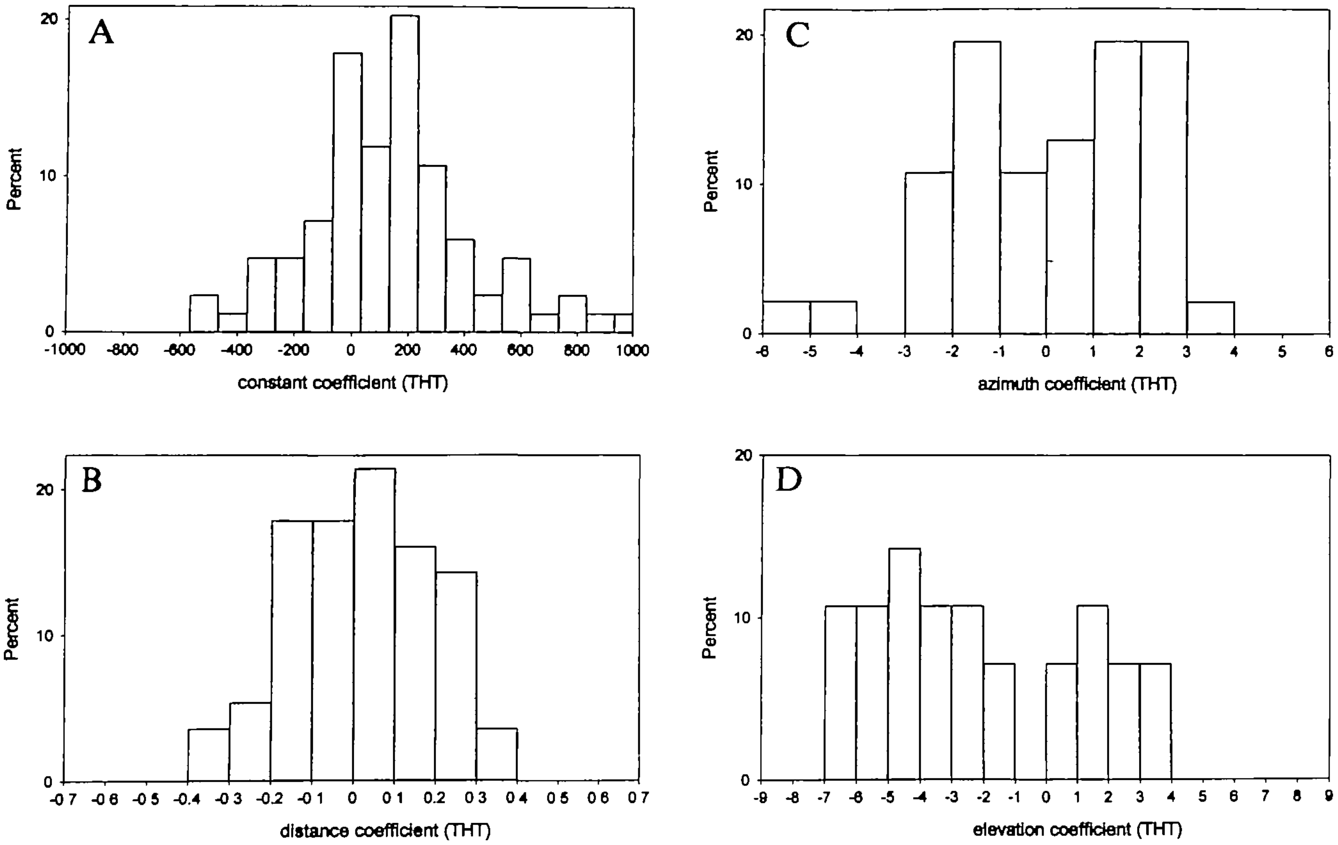

Figure 6. Frequency distribution of the regression parameters for THT activity. Statistically significant coefficients are from the linear model of final wrist position in shoulder-centered spherical coordinates.

of THT discharge as a function of wrist position (in shoulder-centered spherical coordinates). We found that 95% of the total sample variance is explained by the first eigenvector alone (aligned with one coordinate axis) in 66% of all significant neurons, and by the first two eigenvectors (each aligned with a different coordinate axis) in 26% of the neurons. All three spatial eigenvectors (coordinates) are necessary to account for the experimental variance in only 9% of the neurons.

To compare the results across neurons having different levels of activity, we normalized the absolute (unsigned) values of the coefficients of the partial multivariate regressions (see Materials and Methods). The normalized coefficients express the relative gain of each spatial parameter in any given cell and represent its homogeneous coordinates in 3D space. A schematic diagram in the homogeneous spherangular coordinates of the wrist is shown in Figure 7. The closer is a cell to one vertex of the triangle, the greater the relative contribution of the corresponding spatial coordinate and the smaller that of the two other coordinates. By contrast, the closer is the cell to the center of the triangle, the more evenly weighted are the relative contributions of all spatial coordinates.

The histogram of the distribution of all significant neurons over the base of homogeneous coordinates is plotted in Figure 8*A*. The coordinates have been discretized in 0.1 unit intervals. The height of the prisms is proportional to the number of cells whose coordinates fall in a given interval. Most cells are tightly clustered around the vertices of the triangle, indicating that they are much more related to one spatial parameter than to the two others. The proportion of neurons with one homogeneous coordinate > 0.7 is 34% for distance, 17% for azimuth, and 17% for elevation. Similar results were obtained for movement (MT) activity (Fig. 8*B*), as described in a following section.

Spherangular coordinates have been used in Figure 8 but similar clusters are observed when spherical or Cartesian coordinates are used to describe wrist position. Clustering holds also when the nonlinear models described above are used instead of the linear model, each coordinate axis now including both linear and nonlinear terms. On the other hand, clustering becomes less evident when all the terms of the regression are included irrespective of whether they contribute to the experimental variance of neural discharge (see Materials

Table 2
Regression models for THT activity

			Shoulder		Eyes	
Coordinates	Model	*n*	%	*R*	%	*R*
Cartesian	Linear	3	64	0.729		
Cartesian	Nonlinear	9	54	0.888		
Spherical	Linear	3	64	0.739	67	0.743
Spherical	Nonlinear	9	52	0.892	60	0.892
Spherangular	Linear	3	66	0.740		
Spherangular	Nonlinear	9	54	0.891		
Angular	Linear	4	64	0.790		
Angular	Nonlinear	12	54	0.952		

Data are correlations of THT mean discharge with final limb position. For each regression, the coordinate system, model order, number of spatial parameters, percentage of fitted neurons (*F* test, $\alpha = 0.05$), and mean correlation coefficient are indicated. Nonlinear models included linear, quadratic, and cubic terms. For spherical coordinates, results with the origin at the shoulder and eyes are reported.

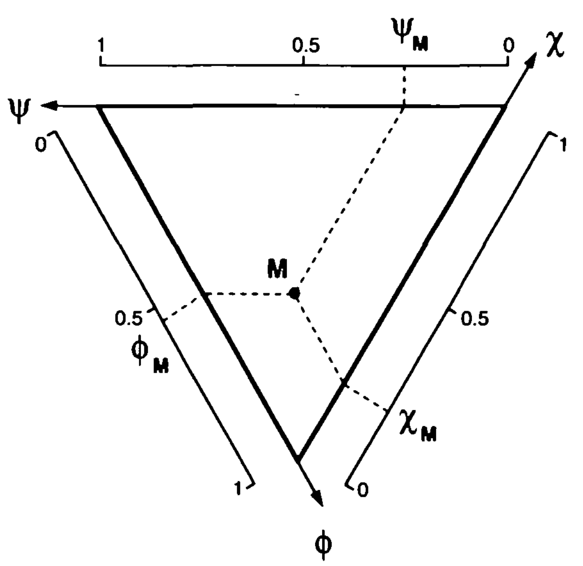

Figure 7. Schematic diagram of the homogeneous coordinates of neural activity. Absolute values of the coefficients a_i of linear regression in spherangular coordinates were normalized according to $a_i^* = |a_i|/\Sigma_j|a_j|$, $i, j = 1, 3$. Values of a_i^* range from 0 (null contribution) to 1 (100% contribution) and express the relative gain of each spatial parameter in any given cell. Increasing values of a_i^* are plotted from top to bottom on the *left side* of the triangle for distance (ϕ), from bottom to top on the *right side* of the triangle for azimuth (χ), and from right to left on the *top side* of the triangle for elevation (ψ). The location of an arbitrary neuron *M* on this triangle is defined by its homogeneous coordinates ϕ_M, χ_M, ψ_M. It corresponds to the point of intersection of the three lines originating from these coordinates. Each of these lines is drawn parallel to the next contiguous coordinate axis in the clockwise direction.

and Methods). Terms that do not account for statistically significant amounts of variance are scattered throughout 3D space.

Activity of Area 5 Neurons during Movement

The mean activity during movement was analyzed according to two different models: (1) vector code of movement direction and (2) positional code in body-centered coordinates.

Directional Properties in Each Part of the Workspace

Analysis was carried out according to the procedures previously described (Georgopoulos et al., 1982; Schwartz et al., 1988; Caminiti et al., 1990, 1991). Essentially, the mean firing rate during MT was fitted with a cosine function of the angle between the direction of movement and the cell's PD in each cube separately. We found that 52% of the neurons were fitted by this model in either the left, the center, or the right cube. However, only 22% of the neurons were fitted in all three cubes, 27% in two cubes, and 34% in one cube. The proportions of directional neurons were even lower during RT: 12%, 24%, and 32% in three, two, and one cube, respectively. Because the main goal of the present study was to characterize the directional properties across the workspace, only those cells that were directionally tuned in at least two parts of space were further analyzed.

When the PDs computed in different parts of the workspace are compared, one finds that they are not invariant, as is also the case in M1 (Caminiti et al., 1990) and PMd (Caminiti et al., 1991). The rotations of PDs in space are visualized in Figure 9. Clearly, the orientation of PDs change markedly for movements performed in different parts of the workspace. The direction and amount of rotation are highly idiosyncratic to each given neuron. The absolute angular differences between the PD spatial orientation in the left cube and that in the right cube ranged up to 140° over the ensemble of neurons (circular mean = 50°).[1]

A different question concerns the spatial coherence between the directional tuning (as expressed by the PD) of a given neuron during movement and the positional gradient of the same neuron during static posture. Spatial coherence was estimated in the following way. The static positional gradient **G** was computed from the linear regression of THT activity on the Cartesian coordinates of the hand at all targets (Kettner et al., 1988). **G** is a vector in the direction of the maximum change in neuronal discharge related to target positions. We then computed the cosine of the angle (inner product) between **G** and PD of the same neuron. The cosine is 1 when these two vectors are in the same direction, −1 when they are oppositely directed, and 0 when they are orthogonal. The results for the three cubes are plotted in Figure 10. For each cell the PD in one or more of the three cubes was compared with the positional gradient computed over the entire workspace. It can be noted that the spatial coherence is highly variable among neurons, with cosine values spanning the full range between 1 and −1.

Positional Properties in All Parts of the Workspace

The appeal of the directional model considered in the previous section is based on its applicability to many different cortical and subcortical areas (see Georgopoulos, 1991). However, the percentage of area 5 neurons directionally tuned in all three parts of the workspace was rather low. Moreover, the PDs of most such neurons changed substantially from one part to the other of the workspace. Finally, the spatial coherence between the PD and the static positional gradient was highly variable among neurons. We have assessed, therefore, an alternative model to account for the measured changes in neural activity during movement. According to this model, a given neuron is characterized by just one set of tuning parameters that apply globally to different parts of the workspace, independently of initial hand position or target location. In this model, target and hand location are neurally encoded relative to a fixed origin. We found that the model predicts well the movement discharge of many neurons throughout the tested workspace. Moreover, the tuning of most cells during movement, as predicted by the positional model, was coherent with the corresponding tuning during stationary posture at the targets.

MT activity was fitted by means of a linear combination of the initial wrist position and of the difference between the final and initial position (Eq. 3). Sixty-seven percent of the neurons were fitted by this model, with a mean *R* of 0.833 in shoulder-centered spherical coordinates. The results were not very different in the other coordinate systems we have considered, as was the case for THT activity. For instance, the percentage of fitted neurons and the corresponding mean *R* were 66% and 0.815 in Cartesian coordinates, 65% and 0.824 in spherangular coordinates, and 59% and 0.898 in angular coordinates.

The model used to fit MT activity was broad, insofar as it could account for both positional and directional properties. In fact, the relative weight of these terms turned out to be quite different. Most neurons were related essentially to final wrist position. This was demonstrated using two different procedures (see Materials and Methods). First, in the model of Equation 3 the coefficients of initial position deviated by <10% from the corresponding coefficients involving the difference between final and initial position in 59% of the cells. Thus, the initial position terms tended to null themselves by algebraic subtraction, leaving the final position terms as the dominant terms in the regression. Second, a model involving a linear combination of initial position, final position, and dif-

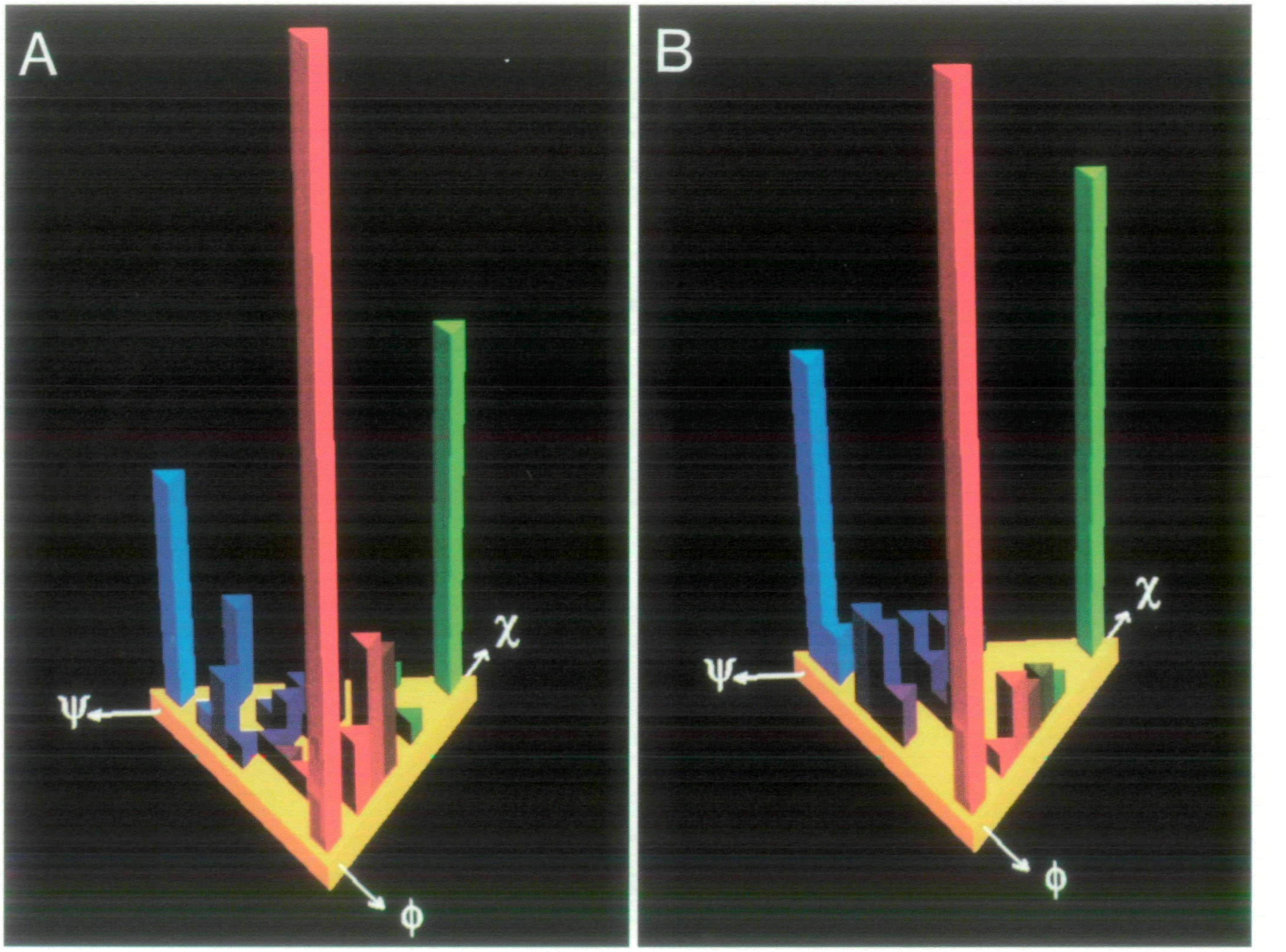

Figure 8. Histograms of the distribution of all neurons over the base of homogeneous coordinates. The coordinates have been discretized in 0.1 unit intervals. The height of the prisms is proportional to the number of cells whose coordinates fall in a given interval. Prisms at the azimuthal vertex (coordinates 1, 0, 0) are in *green*, at the elevation vertex (0, 1, 0) in *blue*, and at the distance vertex (0, 0, 1) in *red*. Prisms at intermediate locations are color coded in proportion to the distance from each vertex. *A*, THT activity; *B*, MT activity.

ference between the final and initial position was separately assessed. Partial models were then constructed by removing one term at a time from the complete best-fitting model and the residual variance was tested (Morrison, 1990). We found that the residual variance of partial models that included only the terms in final position was the same (F test, $\alpha = 0.05$) as that of the complete model in 62% of the neurons. According to the same procedure, 5% of the neurons were related significantly to initial position only, 6% to the difference between final and initial position, and 27% required all the terms of the complete model.

Families of Neurons. The neurons plotted in Figure 11 are examples of the most numerous group under the present experimental conditions. Their mean MT activity was related quasi-monotonically to the changes in final wrist position through all points of the tested workspace. For the sake of comparison, we have plotted the same six neurons whose discharge during THT has been plotted in Figure 5. As in that figure, the corners of the wire frames indicate the mean position of the wrist at the end of the movement to the corresponding target. The gray bars adjacent to each corner indicate the firing rate averaged during MT across all trials to that target. By comparing the results illustrated in Figure 11 with those in Figure 5, it can be noted that the activity recorded in each such neuron during movement is modulated in the same direction as the activity recorded during stationary posture. Thus, the mean neural activity is related to the azimuth of wrist position in *A* and *B*, to distance in *C* and *D*, and to elevation in *E* and *F*. The black bars indicate the firing rate predicted by a linear model of final wrist position in shoulder-centered spherical coordinates (i.e., the same model used for THT activity in Fig. 5). This model predicts the actual discharge of these neurons reasonably well throughout the workspace, as can be appreciated by comparing the gray bars (data) with the corresponding black bars (model). The regression parameters are reported in the figure legend. It is noteworthy that they are similar to those computed for THT activity (see Fig. 5 legend), indicating that the relationship of MT activity with the spatial coordinates of the wrist is coherent with that of THT activity not only qualitatively but also quantitatively. When THT activity was related nonlinearly with wrist position, so was MT activity (e.g., neuron *F* in Figs. 5, 11).

The subpopulation of neurons related to final distance deserves further consideration, in view of their relevance to the issue of the coordinate system putatively involved in the en-

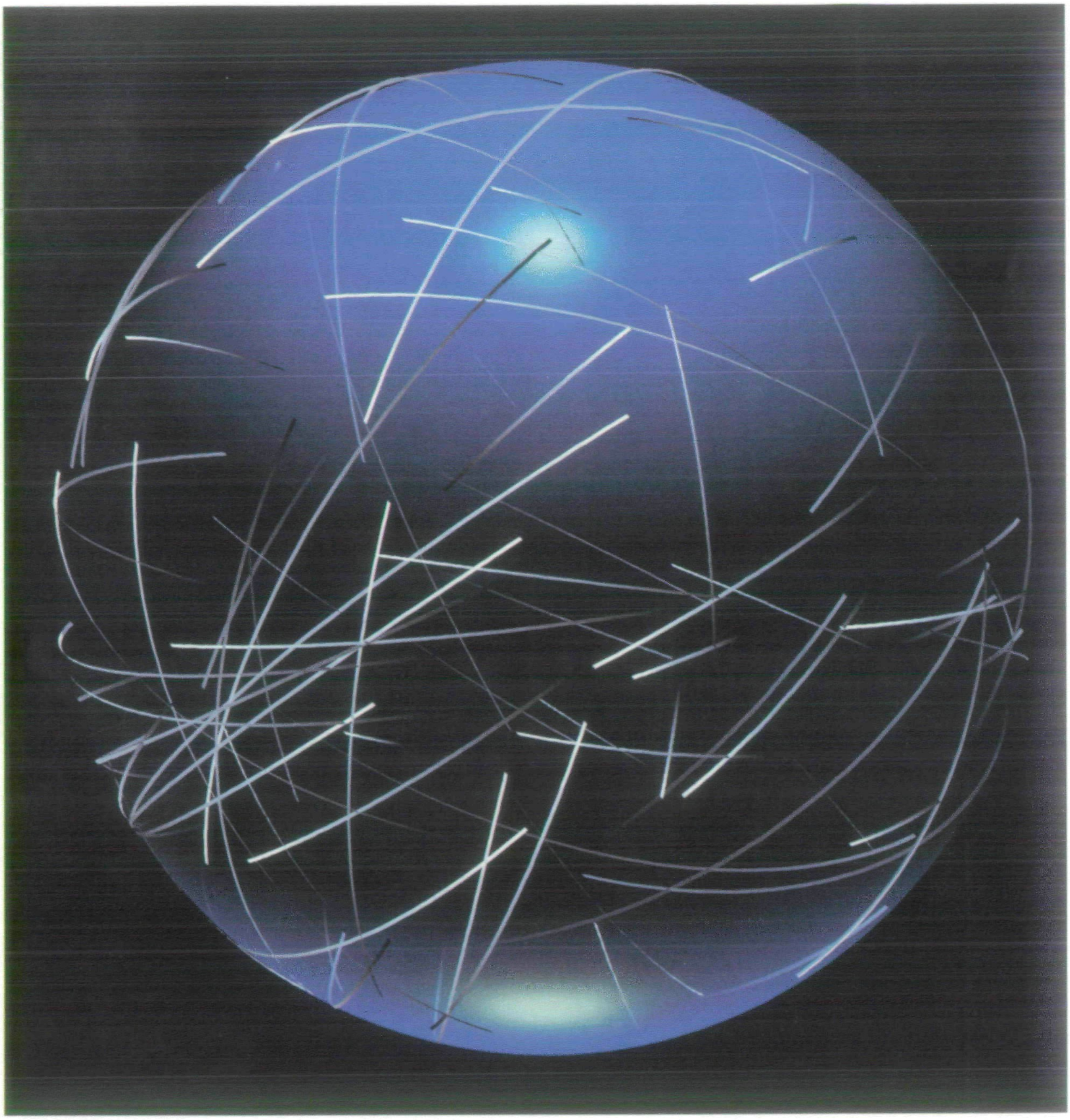

Figure 9. Apparent rotations of the PDs for movements performed in different parts of the workspace. PDs are unit length vectors with origin at the center and tip on the *solid sphere.* Each *white curve* ("comet") on the surface of the sphere represents the apparent trajectory traced by the tip of the PD vector of an individual neuron through workspace. The *darkest part* of the comet ("tail") corresponds to the orientation of the PD computed in the right cube, whereas the *brightest part* of the comet ("head") corresponds to the orientation of the PD in the left cube.

coding of limb movement in area 5. Because the targets were placed along parallel rows, the distance coordinate (x) takes only two values in the Cartesian coordinate system (parallel to the setup), one value for near targets and another one for far targets (see Fig. 1*a*). One would then expect a bimodal distribution of neural activity in this Cartesian frame. By contrast, the distance coordinate (ρ) of the spherical coordinate system varies continuously across the targets (see Fig. 2). Thus, on the near plane, ρ is smallest at the targets immediately in front of the monkey (14 or 23 and 12 or 21) and increases progressively at targets placed more medial (3, 1) or lateral (24, 22) to the monkey. Changes on the far plane are similar, though more limited because the wrist is not protracted in proportion to target distance at the extremes of the workspace (targets 5 and 26). One would then expect a bell-shaped modulation of neural activity along the near plane, with a relative maximum (or minimum) at the central targets placed in front of the monkey. A similar, though less marked, modulation should exist on the far plane. This was indeed the case in most distance-related neurons. Two examples have been plotted in Figure 11, *C* and *D*, and three other examples are shown in Figure 12*A*-*C*. As before, the activity predicted by the final position model in shoulder-centered spherical coordinates is indicated by the black bars. In all these neurons

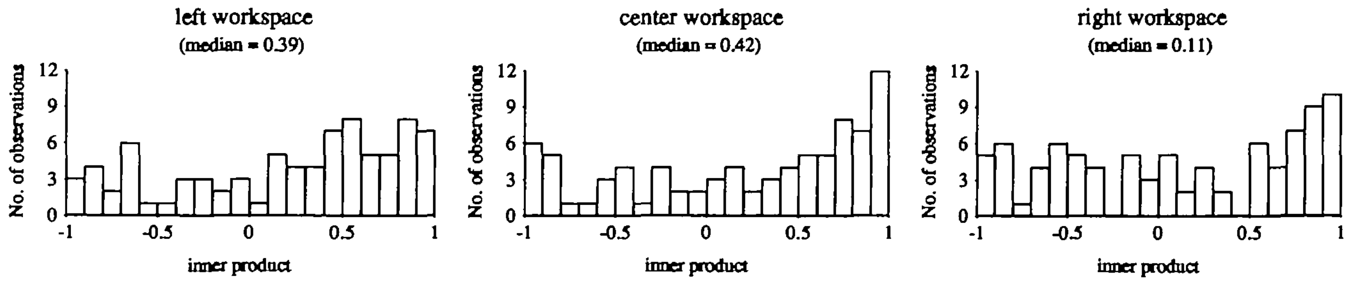

Figure 10. Spatial coherence between the PDs and the positional gradients (*G*). G is a vector in the direction of the maximum change in THT activity throughout the workspace. The cosine of the angle (*inner product*) between G and PD of the same neuron is 1 when these two vectors are in the same direction, −1 when they are oppositely directed, and 0 when they are orthogonal. For each cell the PD in one or more of the three cubes was compared with the positional gradient computed over the entire workspace.

and in 78% of all distance-related neurons ($n = 27$), this model fitted the data better than the same model expressed in Cartesian coordinates. (Seventy-six percent of the distance-related neurons during THT exhibit a better correlation in spherical coordinates than in Cartesian coordinates.)

The neurons plotted in Figure 11, *C* and *D*, and Figure 12*A* are related to distance only. The activity of the neurons of Figure 12, *B* and *C*, instead, is related to both distance and elevation (increasing for increasing distance and decreasing elevation). However, distance effects are clearly dissociable from those of elevation. Elevation neurons are depicted in Figure 11, *E* and *F*, and Figure 12*D*. Their activity is similar on the near and far plane of targets, but varies deeply with their height.

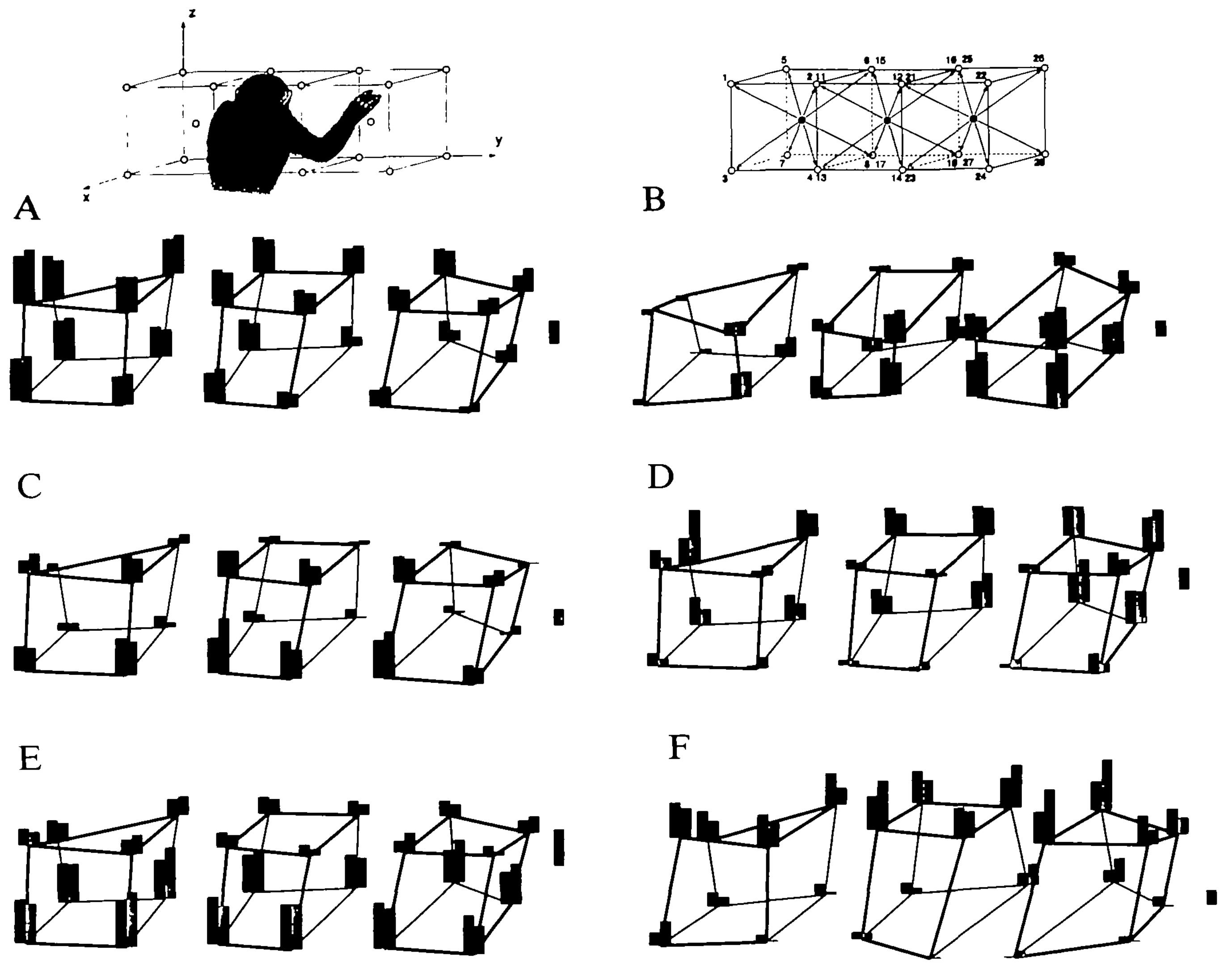

Figure 11. Mean activity of "final position" neurons during movement time (MT). Results are from the same six neurons whose THT discharge has been plotted in the same format in Figure 5. The multiple correlation coefficients (*R*), and the coefficients of the final position terms are, for *A*, (0.838), -4.33χ; *B*, (0.847), $-0.18\rho + 4.45\chi - 5.15\psi$; *C*, (0.799), -0.48ρ; *D*, (0.577), 0.26ρ; *E* (0.834), $-1.21\chi - 7.67\psi$; *F*, (0.554), 14.59ψ.

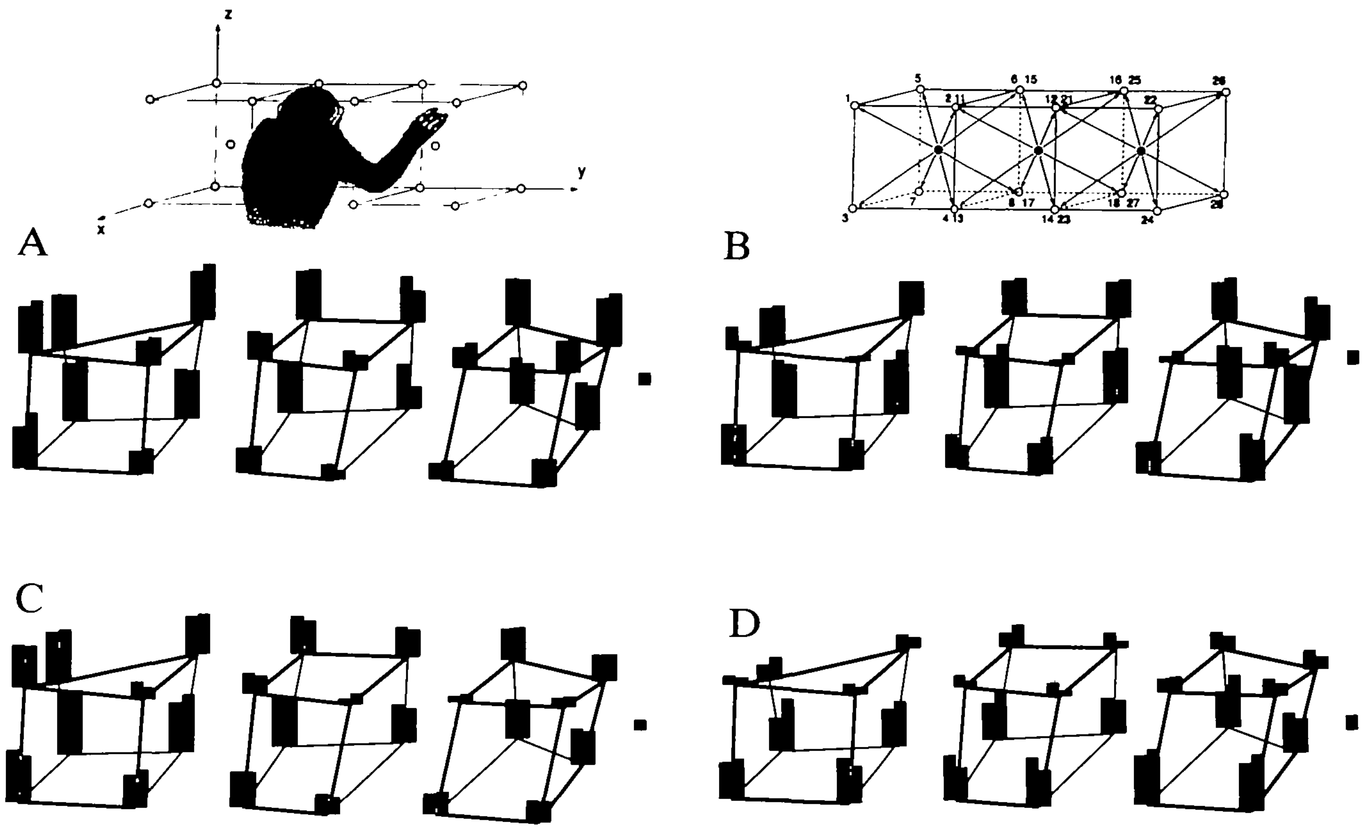

Figure 12. MT activity of four other "final position" neurons. *A*, (0.814), 0.59ρ; *B*, (0.873), $0.13\rho - 5.15\psi$; *C*, (0.950), $0.62\rho - 5.68\chi - 11.89\psi$; *D*, (0.822), -7.79ψ.

As noted above, the movement activity of a proportion of neurons was not explained adequately by a model including final position only. Some examples are shown in Figure 13. Neuron *A* can be defined as "variational," being related to the difference vector between final and initial position. The mean activity of this neuron during MT increased consistently for movements directed to the left and below the starting position for the movements performed in each cube. Thus, the modulation of activity was independent of the initial wrist position and only depended on the relative direction of movement as defined in body-centered coordinates. Accordingly, the correlation coefficient *R* of the model with variational terms only ($M = 0$ in Eq. 3) was 0.923 in this neuron, whereas the *R* for the model in final position was 0.325. (For the sake of comparison, the corresponding *R* values for the "positional" cell illustrated in Fig. 11*A* were 0.250 for the variational model and 0.838 for the final position model.) Note that, in contrast with the "positional" neurons, none of the "variational" neurons exhibited a significant modulation of THT activity with target position (Eq. 2 did not fit the data). The percentage (6%) of "variational" neurons in body-centered coordinates is much lower than the percentage (22%) of directional neurons derived in a previous section by fitting the directional model to the data obtained in each cube separately. This is due to the fact that in the former case the tuning function is assumed to be constant in all three cubes, whereas in the latter case the tuning function is allowed to change and does often change from one cube to the other.

The neurons plotted in Figure 13*B*-*D* were related to both initial position and the difference between final and initial position. Neuron *B* was related to azimuth, neuron *C* to distance, and neuron *D* to both distance and azimuth. The *R* values were 0.842, 0.758, and 0.874 for the complete model in *B*-*D*, respectively, and dropped to 0.634, 0.217, and 0.442 for the final position model, and to 0.063, 0.047, and 0.197 for the variational model.

Further Tests of Positional Factors. Each boundary corner ($n = 8$) between adjacent cubes corresponded to the same target location but was reached from two different movement directions (see Figs. 1*b*, 2). We were then able to compute a *Z* score of the difference between the mean MT discharge for one direction and the MT discharge for the other direction to the same target. Pairwise comparisons were performed for each boundary corner in each neuron. We found that the difference in discharge was not statistically significant ($\alpha = 0.05$) in 58% of all target-neuron combinations, and in at least half of the boundary corners of 70% of the neurons. (The same tests on THT activity yielded 68% and 84% of not significant cases, respectively.)

The overall relations between neural activities associated with these movements are shown in the scatter plots of Figure 14*A* for MT discharge and Figure 14*B* for THT discharge. Each point corresponds to the discharge during two equifinal movements to the same boundary target but reached from two different directions. Movements in a pair were randomly assigned to the abscissa or the ordinate. Both MT and THT activities tended to be similar for equifinal movements; the correlation coefficient was 0.762 ($p < 0.001$, $n = 672$) for MT and 0.847 for THT.

The relevance of final position as a determinant of MT discharge suggests that neural activity during movement is modulated in parallel to the modulation of stationary activity at the targets (THT activity). This point has already been noted in relation with the neurons plotted in Figure 11. To generalize the observation we computed the correlation coefficient between MT and THT activity over all targets ($n = 24$) in each cell ($n = 131$). Figure 15*A* shows the distribution of the correlation coefficients. Of these, 80% were significantly

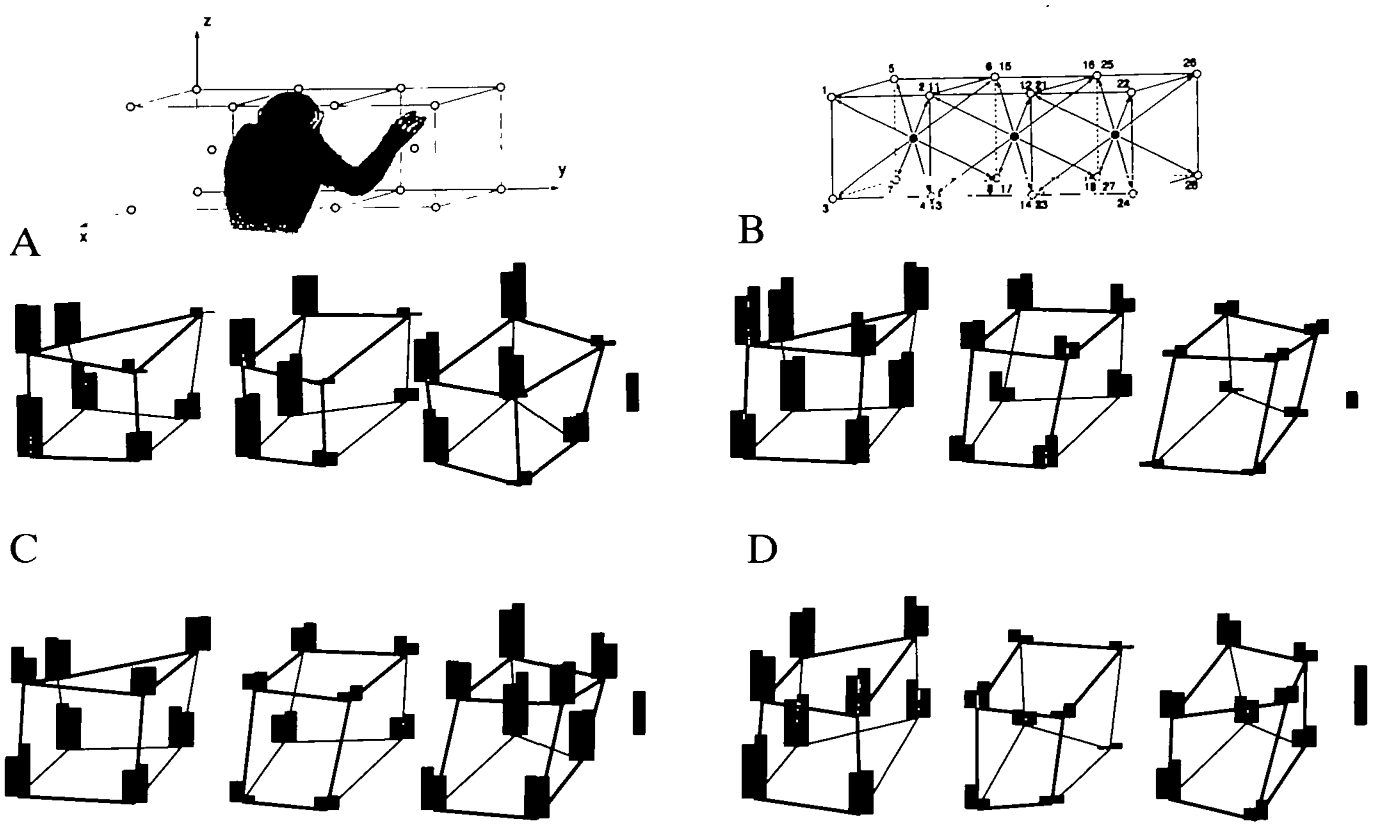

Figure 13. MT activity of four neurons belonging to other classes. *A*, (0.923), $-7.96\Delta\chi - 2.95\Delta\psi$; *B*, (0.842), $-7.16\chi_f - 0.44\Delta\chi$; *C*, (0.758), $0.73\rho_f + 0.06\Delta\rho$; *D*, (0.874), $0.31\rho_f - 3.23\chi_f - 1.46\Delta\chi$.

> 0 ($\alpha = 0.025, R > 0.404$, df = 22). The high degree of MT-THT correlation is not due to the intrinsic autocorrelation of cell activity during different time epochs. For instance, RT activity was poorly correlated with THT activity (Fig. 15*B*): only 26% of the neurons exhibited an RT-THT correlation significantly > 0.

To investigate further the relation between MT and THT activity, the following equation was fitted to the cells with a significant correlation:

$$r(\mathrm{MT}) = a + b\, r(\mathrm{THT}) \qquad (4)$$

Figure 15*C* shows the distribution of the slopes b over these cells. It can be noted that this distribution is centered roughly symmetrically around 1. [Mean values of b and a are 0.975 ± 0.088 ($\pm$SEM) and 35 ± 19, respectively.] Thus, on average, the changes in MT activity are quite similar to the changes in THT activity through the tested workspace. However, MT activity is significantly smaller ($b < 1$) or greater ($b > 1$) than THT activity in a substantial proportion of cells.

Having established the close parallelism between MT and THT activity, we now report a summary of the positional properties expressed by means of the same model of final position (shoulder-centered spherical coordinates) that was used for THT activity (Eq. 2). Figure 16 shows the frequency distribution of the regression parameters over the ensemble of fitted neurons. These distributions are comparable to those obtained for THT activity (see Fig. 6). The spatial coherence between the positional tuning during movement and that during stationary posture is illustrated in Figure 17. For each fitted neuron we computed the cosine of the angle between the vector of the regression coefficients of final position for MT activity and the corresponding vector for THT activity. The cosine was close to 1 in most neurons, indicating almost perfect spatial coherence. This is to be contrasted with the variable spatial coherence existing between PDs and positional gradients (see Fig. 10).

The same type of segregation that we have previously described for the stationary code of limb position applies also to the movement code: different spatial coordinates tend to be segregated in different subpopulations of neurons. The histogram of the distribution of MT activities over the base of homogeneous spherangular coordinates is plotted in Figure 8*B*. As in the case of THT activity (Fig. 8*A*), most cells are tightly clustered around the vertices of the triangle, indicating that they are much more related to one spatial parameter than to the two others. The proportion of neurons with one homogeneous coordinate > 0.7 was 28% for distance, 20% for azimuth, and 16% for elevation.

Positional factors are preeminent in the modulation of area 5 neurons during all time epochs of the task. Thus, RT activity tended to be closely related to CT activity and initial position, in the same manner as MT activity was related to THT activity and final position. The correlation coefficient between RT and CT activity over all targets was statistically significant in 72% of the neurons. The mean value of the regression slope over these cells was 0.986 ± 0.095 ($\pm$SEM). As a consequence, RT activity was poorly related to both MT and THT activity (Fig. 15*B*). However, RT activity was tuned in the same manner as MT activity in the variational neurons (as that of Fig. 13*A*).

Discussion

There are three main findings in our study of dorsal area 5. (1) Many neurons are positionally tuned during both movement and stationary posture. In contrast to frontal areas (Schwartz et al., 1988; Caminiti et al., 1990, 1991), relatively few neurons seem to be tuned to movement direction per se. (2) Positional tuning is defined in a reference frame with the

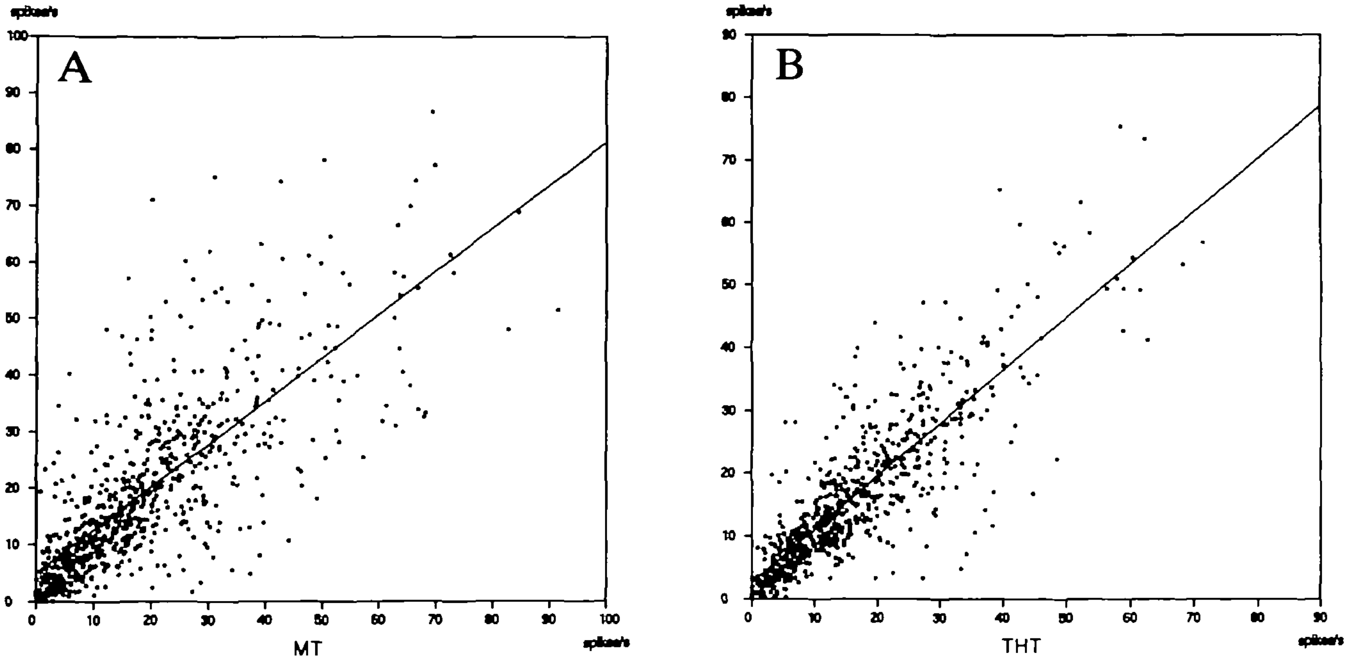

Figure 14. Scatter plots of cell activity during equifinal movements. Boundary targets were reached from two different directions. Movements in a pair were randomly assigned to the abscissa or the ordinate. *A*, MT activity; *B*, THT activity.

same origin for movements performed in different parts of the workspace. This reference frame is presumably centered on the body. (3) Each spatial coordinate could be separately encoded in a distinct subpopulation of neurons.

Positional versus Directional Tuning Properties

An orderly, linear relation was found in previous studies between the mean activity of area 5 cells during target holding and the actively maintained position of the hand in one central region of 2D space (Georgopoulos et al., 1984; Georgopoulos and Massey, 1985). The results of the present study extend those observations to a much larger range of stationary postures, associated with the reaching to targets located in three different regions of 3D space. The percentage of positional neurons (as determined by linear regression of neural activity on wrist position) is similar (about 60% of the sample) to that previously reported in 2D studies (Georgopoulos et al., 1984). We found that the same regression parameters fitted both THT activity and CT activity of most neurons for all targets. This implies that the static neural activity is correlated with the corresponding wrist position throughout the tested workspace, irrespective of whether stationary maintenance of posture precedes or follows a movement. Nonlinear models including linear, quadratic, and cubic terms of wrist position fitted the neural discharge better than the simple linear model. However, the magnitude of local nonlinearities is generally small compared to the linear slope of the regression. Of course, one cannot extrapolate this quasi-monotonic behavior outside the tested workspace. It is quite possible that activity saturates or falls off there.

We have analyzed the activity of area 5 neurons during movement using two different approaches. First, directional tuning was assessed separately in each one of the three parts of the workspace according to the classical cosine model (see Schwartz et al., 1988; Caminiti et al., 1990). We found that a relatively low (22%) proportion of neurons is fitted by this model in all three cubes. This proportion is much lower than that obtained in M1 (75% of the neurons, Caminiti et al., 1990) and in PMd (77%, Caminiti et al., 1991) using the same task and apparatus. On the other hand, the proportion of neurons (52%) that are fitted in either one of the three cubes is not very different from that (62%) reported in a previous study of area 5 using only one central region of 2D space (Kalaska et al., 1983) For those neurons that are directionally tuned in both the left and the right cube, one can compare the respective orientation of the PDs. They differ by as much as 140°, with a 50° mean difference. Not only the magnitude, but also the direction of change in PD orientation is highly idiosyncratic to each given neuron and has an erratic orientation in space (see Fig. 9). Consequently, the spatial coherence between the directional tuning of a given neuron during movement and the positional gradient of the same neuron during stationary posture is also highly variable among neurons, in agreement with a previous report of 2D reaching movements (Georgopoulos and Massey, 1985).

Although we see no reason to reject this directional model, we believe that the second model we have considered provides a more plausible account of the physiological properties of area 5 neurons. This model assumes that the tuning function of a given neuron is the same in different parts of the workspace, instead of changing across space as implied by the previous model. The present model is more general insofar as it encompasses both positional and variational terms. Sixty-seven percent of the neurons are fitted by the model. The relative weight of positional and variational terms is quite different in different neurons. On this basis we have been able to distinguish different classes of neurons. Sixty-two percent of the fitted neurons are related essentially to final position, 5% to initial position, 6% to the variational terms, and 27% to both initial position and the variational terms.

The movement activity of the first class of neurons is related quasi-monotonically to the position of the wrist at the peripheral target throughout the tested workspace. The weight of positional factors is underscored by the observation that the activity of these neurons during movements directed toward the boundary targets is largely independent of the specific direction of movement. The simple linear model on final position fits both THT activity and MT activity of a given

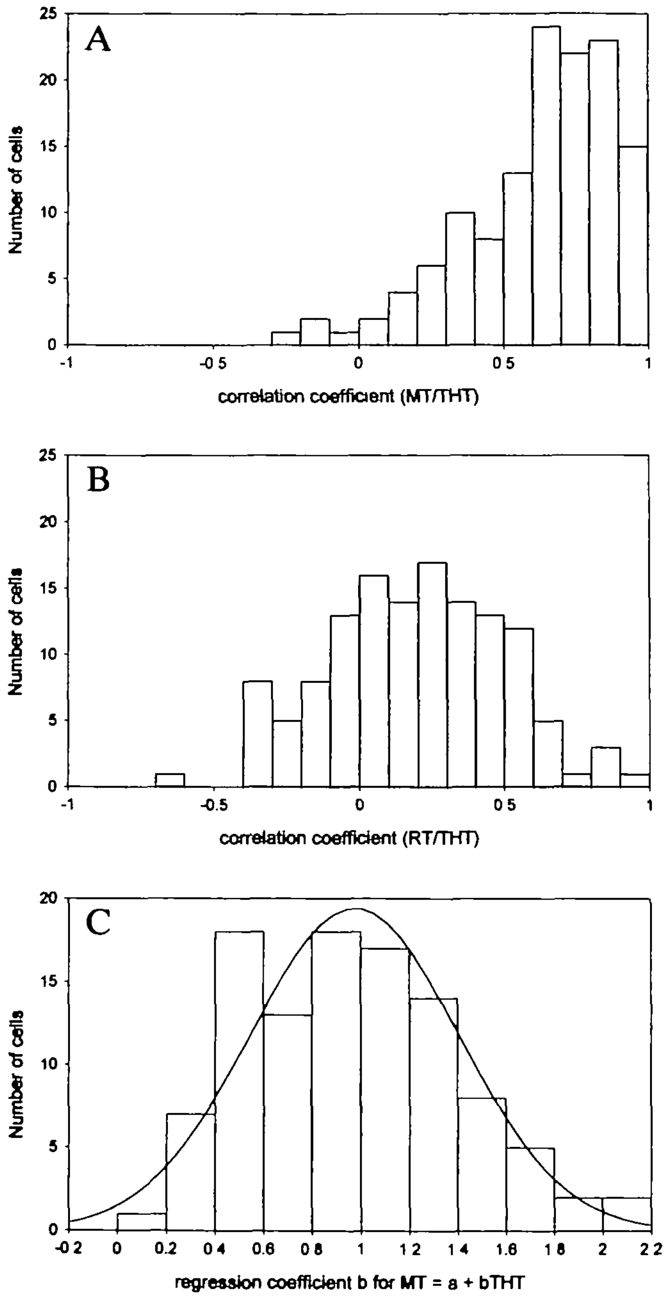

Figure 15. Distribution of the correlation coefficients between MT and THT activity (*A*) and between RT and THT activity (*B*) over all neurons ($n = 131$). *C*, Distribution of the slopes of the linear regression of MT activity over THT activity over all neurons ($n = 105$) with a significant correlation. Best-fitting gaussian curve is superimposed on the distribution.

neuron with similar regression coefficients. Accordingly, the spatial congruence between the positional code during stationary posture and that during movement is generally very high, in contrast with the variable association between PDs and positional gradients discussed above.

The properties of the other classes of neurons are described also by a fixed tuning function throughout the workspace. Movement activity of "initial position" neurons does not change relative to the starting point. "Variational" neurons are related to the difference vector between final and initial position, that is, to the motor error. The description of the activity of the neurons related to both initial position and the variational terms is more difficult. This activity could be correlated with positions (via-points) located along the direction of movement. All classes of neurons, except that of "variational" neurons, show a significant correlation of THT activity with final position; "variational" neurons lack these static postural properties.

The boundaries between these classes are not always rigidly defined. A taxonomy of area 5 neurons based on discrete criteria is affected by some degree of arbitrariness, because their properties vary probably along a continuum. On the other hand, there exist some analogies between the classes we have described and those identified in previous studies of area 5 based on different criteria (Mountcastle et al., 1975; Chapman et al., 1984; Kalaska et al., 1990; Burbaud et al., 1991). For instance, Kalaska et al. (1990) identified "tonic" neurons characterized by ramplike changes in movement activity whose intensity is correlated with arm posture. In contrast, "phasic" neurons showed directionally tuned phasic changes prior to or during movement but little or no variation in tonic activity at target holding. "Phasic-tonic" neurons have intermediate properties. A similar heterogeneity of the neural responses associated with movement has been also emphasized in other studies of area 5 (Mountcastle et al., 1975; Chapman et al., 1984; Kalaska et al., 1990; Burbaud et al., 1991).

One has to be very cautious in interpreting neural data during movement. The exact nature of the signals involved cannot be assessed in the absence of a correlation between the time-varying changes in neural activity and the corresponding changes in limb kinematics. Nevertheless, a few considerations are in order. Movement activity can be thought of as composed of a combination of static and dynamic factors (Georgopoulos and Massey, 1985; Kettner et al., 1988). Static factors reflect a direct relationship with limb position, whereas dynamic factors encompass all nonstatic effects. An approximate estimate of their relative contribution is obtained by regressing movement activity on target-holding activity (Kettner et al., 1988). In about 50% of the cells the slope of this relationship is ≤ 1, indicating a large predominance of static positional effects (Fig. 15). Dynamic effects are not negligible in the remaining cells. Their exact nature remains to be determined, but velocity-dependent signals most likely play an important role (Thach, 1978; Schwartz, 1994).

The described relationships with limb position presumably reflect limb kinematics, rather than kinetics, in agreement with previous studies of area 5 (Kalaska et al., 1990). In fact, the monotonic modulation of neural activity with limb position departs from the nonmonotonic relation that characterizes muscle activity at shoulder and elbow joints (Flanders and Soechting, 1990). Some neural activity may reflect current position of the limb, as signaled by peripheral feedbacks or efferent copy of motor commands: CT and RT activity related to starting point, MT activity related to via-points, and THT activity related to final point. MT activity related to final point, however, may reflect a preplanned desired position or command function rather than current kinematics (Mountcastle et al., 1975; Hocherman and Wise, 1991). Eye position signals might theoretically play a role.

According to some present theories on trajectory formation, lawful characteristics of reaching kinematics can be accounted for by assuming that a few spatial landmarks including start and final point are centrally specified. Time-varying kinematics may not need to be planned explicitly, emerging from minimum principles (Flash and Hogan, 1985; Bizzi et al., 1992; Hirayama et al., 1993). The λ-model predicts that central commands specifying the equilibrium point change monotonically reaching the final point well before the end of the movement (Feldman and Levin, 1995). According to an alternative model (Bullock and Grossberg, 1988), three types of signals are computed in the brain: a target-position command

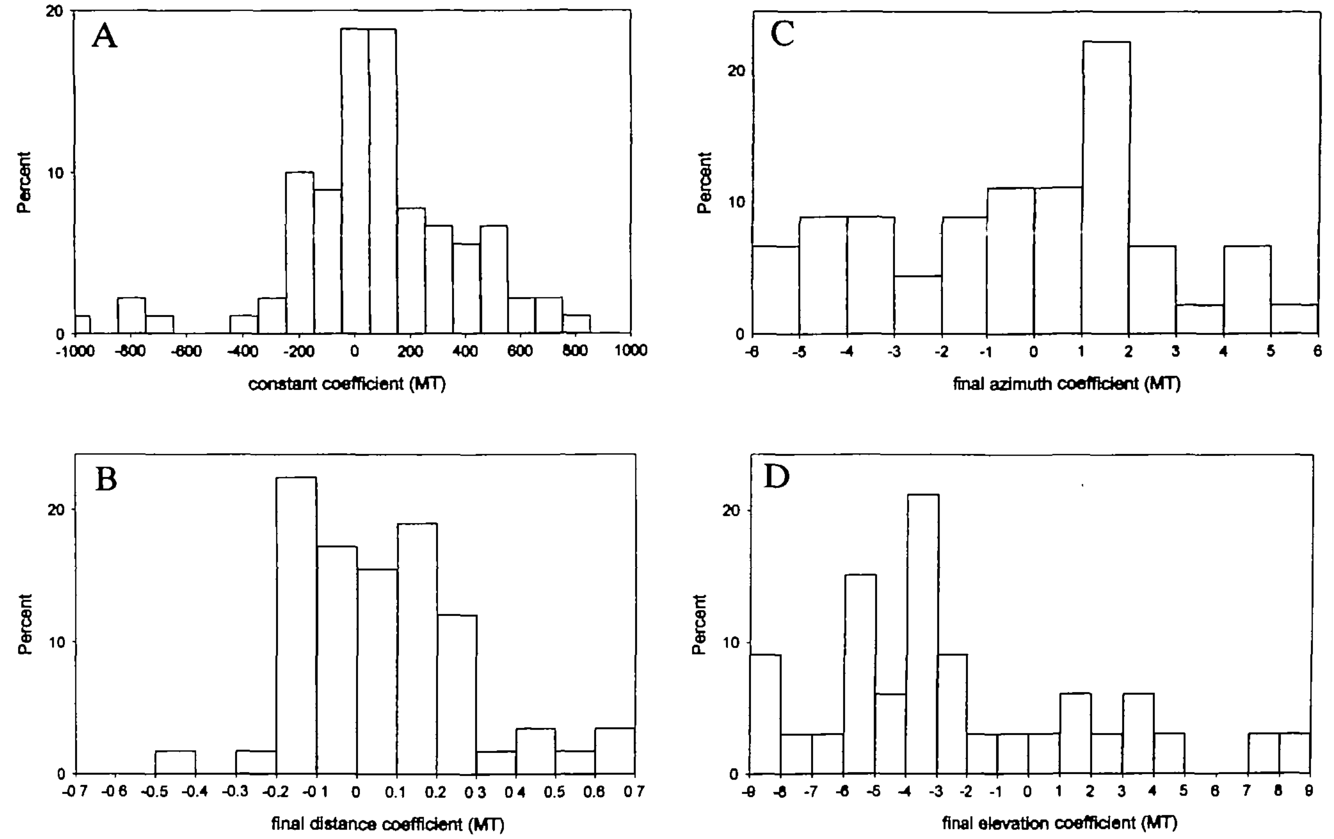

Figure 16. Frequency distribution of the regression parameters for MT activity. Statistically significant coefficients are from the linear model of final wrist position in shoulder-centered spherical coordinates.

(TPC), which is switched on once and for all at movement inception; a present-position command (PPC), which is continuously updated until it matches TPC; and a difference vector (DV) between TPC and PPC. The diversity of functional properties observed in area 5 neurons is compatible with these and other views emerging from psychophysical and modeling studies.

The Issue of Body-Centered Coordinate Systems

We have shown that the activity of area 5 neurons is related to changes of limb position in a reference frame with the same origin for movements performed in different parts of the workspace. Neural modulation was explained better in body-centered coordinate systems (spherical, spherangular, and angular) than in a Cartesian coordinate system parallel to the laboratory frame. We have been unable to determine whether the origin of the body-centered coordinate system is located at the eyes, body midline, or shoulder, because the monkeys performed the reaching movements with head fixed and with limited motion of the torso and shoulder. Nor could we determine whether limb position is neurally encoded in terms of the global wrist coordinates or in terms of the individual orientation angles of both upper arm and forearm. Monkeys performed highly stereotyped movements, wrist position covarying tightly with the orientation angles of the upper arm and forearm. The fact that the latter provide a better fit of the neural data could be due simply to the greater number of parameters (degrees of freedom) used in the model.

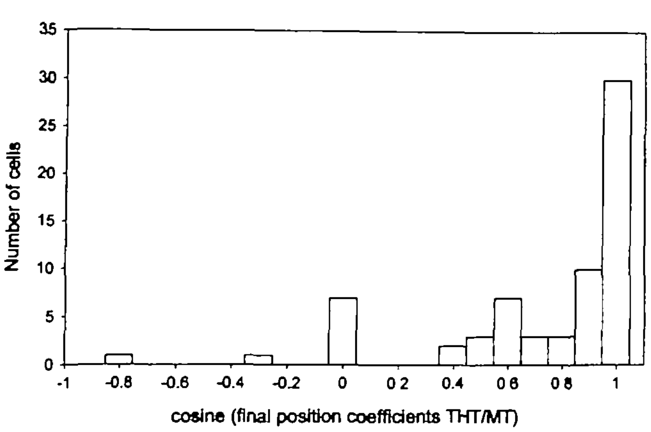

Figure 17. Spatial coherence between the positional tuning during movement and that during static posture. The cosine of the angle between the vector of the regression coefficients of final position for MT activity and the corresponding vector for THT activity were computed for all fitted neurons (*n* = 67).

The main point about the present findings is that neural activity during posture and movement can be explained in coordinate systems that are not related exclusively to the geometry of the somatosensory and motor apparatus, but depend on multisensory integration and central processing. Thus, both the spherical coordinates of the wrist (azimuth, elevation, distance) and the orientation angles of the limb (yaw, elevation) require to be defined the hybrid combination of a reference external to the limb with the intrinsic somatosensory information about limb configuration (Soechting et al., 1986). This reference could correspond to the vertical, as sensed by the vestibular apparatus, or as estimated by visual and somatosensory cues as an idiotropic vector. The finding that the activity of several neurons in area 5 encodes the final point during movement and stationary posture in a coherent manner suggests that information about target location is transformed into the same body-centered coordinate system used to encode limb position (Soechting and Flanders, 1989a). Alignment in register of information from multiple sensors and destined to multiple motor effectors is one important *raison d'être* of intermediate processing stages in hybrid reference frames (Grobstein, 1988; Masino and Knudsen, 1990; Flanders et al., 1992; Carrozzo and Lacquaniti, 1994). Intermediate representations are useful both to produce output signals and to compare reafferent signals with efferent copies of such output (Bullock and Grossberg, 1988).

The known physiological characteristics of area 5 neurons are compatible with the generation of positional signals in body-centered coordinates. Thus, somesthetic receptive fields are generally large, often multimodal and multisegmental (Duffy and Burchfiel, 1971; Sakata et al., 1973; Mountcastle et al., 1975; Burbaud et al., 1991). As to the source of the vertical reference, area 5 is connected with area 2, which in turn receives vestibular inputs (in addition to parietoinsular PIVC region; see Grusser et al., 1990). Alternatively, the reference could correspond to the body sagittal axis. Several neurons in area 5 have receptive fields encompassing both chest and shoulder (Burbaud et al., 1991).

Parcellation of Spatial Information in Area 5 Neurons

A key issue in understanding distributed representations of space in the brain is given by the statistical properties of population ensembles (see Georgopoulos et al., 1988). A consistent observation concerning the vector code of movement direction in motor and premotor cortex has been that the PDs of single cells are distributed uniformly throughout space (Georgopoulos et al., 1988; Caminiti et al., 1990, 1991). This distribution is deemed important for the population code of movement direction by coarsely tuned neurons (Georgopoulos et al., 1988; Burnod et al., 1992).

By contrast, the positional code we found in area 5 neurons does not seem to be uniform in 3D space. When the neurons are classified on the basis of the relative contribution of azimuth, elevation, and distance, most of them (about 70%) cluster around the cardinal spatial axes for both THT and MT activity (Fig. 8). It should be noted, however, that clustering is less evident when the terms that do not account for statistically significant amounts of variance are included also. Pending the acquisition of a larger data sample, we put forth the hypothesis that each spatial coordinate could be encoded in a different subpopulation of neurons. Interestingly, a nonuniform distribution of PDs has been previously reported in a 2D study of area 5 by Kalaska et al. (1983); their Figure 4*A* shows that there is a higher percentage of cells with PDs aligned with the sagittal and frontal axes, corresponding to distance and azimuth, respectively (elevation was not tested).

Segregation of different spatial dimensions has been previously described at several sites of the CNS. For example, the visual responses of distinct populations of neurons in the accessory optic system, inferior olive, and cerebellar flocculus are tuned around the axes of each semicircular canal (Simpson et al., 1988). Horizontal and vertical rotations of the head are controlled by distinct neural circuits in the optic tectum of the owl (Masino and Knudsen, 1990). A proportion of eye-position neurons in area 7a are monotonically tuned along either the horizontal, or the vertical, or the depth axis of gaze (Sakata et al., 1980; Andersen et al., 1990).

What is the functional significance of segregating the information about distance, elevation, and azimuth of hand movements in distinct subpopulations of neurons? Neural parcellation could be a correlate of the psychophysical observation that these spatial parameters are processed in parallel and largely independent of each other (Flanders et al., 1992). Thus, pointing errors in distance are distinct from the errors in azimuth and elevation in man (Soechting and Flanders, 1989a,b; Gordon et al., 1994). Also, the central processing time involved in programming movement direction is different from that involved in programming movement distance (Rosenbaum, 1980). Projecting the spatial information onto separate axes of neural coding could be important for sensorimotor coordination, because information related to motor commands could be matched more easily with incoming sensory feedbacks. Spatial axes that result from a hybrid combination of sensory and motor axes would be best suited to accomplish this matching process (Carrozzo and Lacquaniti, 1994).

Although spatial information could be parcellated at the level of single neurons, the complete information about limb position could still be reconstructed by simple summation of the individual contributions over a population of neurons, because the spatial coefficients are distributed symmetrically in the positive and negative direction (Figs. 6, 16). This can be demonstrated by using a neural network model. A layered neural network whose intermediate layer contains positionally tuned neurons can be trained to generate the position of the hand in body-centered coordinates. Global reconstruction of limb position could take place either inside or outside area 5.

It remains to be seen whether the analysis we have applied here to area 5 neurons can discriminate regional differences with M1 and PMd. There are reasons to believe so. Functional characteristics of arm-related neurons are partially different in frontal and parietal cortices. In area 5, static positional tuning is predominant and relatively few cells are directionally tuned in all parts of workspace. By contrast, in M1 and PMd, dynamic factors are large (Kettner et al., 1988) and the percentage of directionally tuned neurons is much greater than in area 5 (Caminiti et al., 1990, 1991). Area 5 is extensively interconnected with M1 and the border region M1/PMd (Johnson et al., 1993, 1995). One might then speculate that these regions form a network for the coordinate transformations involved in movement generation.

Notes

We thank M. Carrozzo for help with computer graphics and L. Chiumiento for artwork. We also thank Drs. Y. Burnod, A. P. Georgopoulos, P. B. Johnson, J. F. Kalaska, G. Rizzolatti, and two anonymous reviewers for numerous helpful comments on an earlier version of the manuscript. This work was partially supported by grants from the ESPRIT Basic Research (MUCOM 2, 6615), European Neuroscience Programme, and Human Capital and Mobility (ERBCHRXCT930266) awarded by the Commission of the European Communities. E.G. and L.B. were supported by Human Capital and Mobility Fellowship ERCBCHBGCT920085.

Address correspondence to Prof. F. Lacquaniti, Sez. Ricerche Fisiologia umana, CNR, Istituto Scientifico S. Lucia, via Ardeatina 306, 00179 Roma (Italy).

1. A spherical regression analysis was performed to determine the rotation necessary to align globally the two populations of PDs obtained in the left cube and in the right cube, respectively (see Caminiti et al., 1990) This rotation had large, statistically significant components around both the z-axis and the y-axis, in contrast with the pure horizontal (z-axis) rotation observed in M1 (Caminiti et al., 1990) and PMd (Caminiti et al., 1991).

References

Andersen RA, Bracewell RM, Barash S, Gnadt JW, Fogassi, L (1990) Eye position effects on visual, memory, and saccade-related activity in areas LIP and 7a of macaque. J Neurosci 10:1176-1196.

Bizzi E, Hogan N, Mussa-Ivaldi FA, Giszter S (1988) Does the nervous system use equilibrium-point control to guide single and multiple joint movements? Behav Brain Sci 15:603-613.

Bullock D, Grossberg S (1988) Neural dynamics of planned arm movements: emergent invariants and speed-accuracy properties during trajectory formation. Psychol Rev 95:49-90.

Burbaud P, Doegle C, Gross C, Bioulac B (1991) A quantitative study of neuronal discharge in area 5, 2, and 4 of the monkey during fast arm movements. J Neurophysiol 66:429-443.

Burnod Y, Grandguillaume P, Otto I, Ferraina S, Johnson PB, Caminiti R (1992) Visuo-motor transformations underlying arm movements toward visual targets: a neural network model of cerebral cortical operations. J Neurosci 12:1435-1453.

Caminiti R, Johnson PB, Urbano A (1990) Making arm movements within different parts of space: dynamics aspects in the primate motor cortex. J Neurosci 10:2039-2058.

Caminiti R, Johnson PB, Galli C, Ferraina S, Burnod Y (1991) Making arm movements within different parts of space: the premotor and motor cortical representation of a coordinate system for reaching to visual targets. J Neurosci 11:1182-1197.

Carrozzo M, Lacquaniti F (1994) A hybrid frame of reference for visuo-manual coordination. Neuroreport 5:453-456.

Chapman CE, Spidalieri C, Lamarre Y (1984) Discharge properties of area 5 neurons during arm movements triggered by sensory stimuli in the monkey. Brain Res 309:63-77.

Cohen DAD, Prud'homme MJL, Kalaska JF (1994) Tactile activity in primate primary somatosensory cortex during active arm movements: correlation with receptive field properties. J Neurophysiol 71:161-172.

Duffy FH, Burchfiel JL (1971) Somatosensory system: organizational hierarchy from single units in monkey area 5. Science 172:273-275.

Feldman AG, Levin MF (1995) Positional frames of reference in motor control. The origin and use. Behav Brain Sci, in press.

Ferraina S, Bianchi L (1994) Posterior parietal cortex: functional properties of neurons in area 5 during an instructed-delay reaching task within different parts of space. Exp Brain Res 99:175-178.

Flanders M, Soechting JF (1990) Arm muscle activation for static forces in three-dimensional space. J Neurophysiol 64:1818-1837.

Flanders M, Tillery SIH, Soechting JF (1992) Early stages in a sensorimotor transformation. Behav Brain Sci 15:309-362.

Flash T, Hogan N (1985) The coordination of arm movements: an experimentally confirmed model. J Neurosci 5:1688-1703.

Fortier PA, Kalaska JF, Smith AM (1989) Cerebellar neuronal activity related to whole-arm reaching movements in the monkey. J Neurophysiol 62:198-211.

Fu Q-G, Suarez JI, Ebner TJ (1993) Neuronal specification of direction and distance during reaching movements in the superior precentral premotor area and primary motor cortex of monkeys. J Neurophysiol 70.2097-2116.

Georgopoulos AP (1991) Higher order motor control. Annu Rev Neurosci 14:361-377.

Georgopoulos AP, Massey JT (1985) Static versus dynamic effects in motor cortex and area 5: comparison during movement time. Behav Brain Res 18:159-166.

Georgopoulos AP, Kalaska JF, Caminiti R, Massey JT (1982) On the relations between the direction of two-dimensional arm movements cell discharge in primate motor cortex. J Neurosci 2:1527-1537.

Georgopoulos AP, Caminiti R, Kalaska JF (1984) Static spatial effects on motor cortex and area 5: quantitative relations in a two-dimensional space. Exp Brain Res 54:446-454.

Georgopoulos AP, Kettner RE, Schwartz AB (1988) Primate motor cortex and free arm movements to visual targets in three-dimensional space. II. Coding of the direction of movement by a neuronal population. J Neurosci 8:2928-2937.

Grobstein P (1988) Between the retinotectal projection and directed movement: topography of a sensorimotor interface. Brain Behav Evol 31:34-48.

Grusser OJ, Pause M, Schreiter U (1990) Localization and responses in the parieto-insular vestibular cortex of awake monkeys (*Macaca fascicularis*). J Physiol (Lond) 430:537-557.

Hirayama M, Kawato M, Jordan MI (1993) The cascade neural network model and a speed-accuracy trade-off of arm movement. J Mot Behav 25:162-174.

Hocherman S, Wise SP (1991) Effects of hand movement path on motor cortical activity in awake, behaving rhesus monkeys. Exp Brain Res 83:285-302.

Jeannerod M (1991) The interaction of visual and proprioceptive cues in controlling reaching movements. In: Motor control: concepts and issues (Humphrey DR, Freund H-J, eds), pp 277-291. Chichester: Wiley.

Johnson PB, Ferraina S, Caminiti R (1993) Cortical networks for visual reaching. Exp Brain Res 87:361-365.

Johnson PB, Ferraina S, Bianchi L, Caminiti R (1995) Cortical networks for visual reaching. Physiological and anatomical organization of frontal and parietal lobe arm regions. Cereb Cortex, in press.

Kalaska JF, Caminiti R, Georgopoulos AP (1983) Cortical mechanisms related to the direction of two-dimensional arm movements: relations in parietal area 5 and comparison with motor cortex. Exp Brain Res 51:247-260.

Kalaska JF, Cohen DAD, Hyde ML, Prud'homme M (1989) A comparison of movement direction-related versus load direction-related activity in primate motor cortex, using a two-dimensional reaching task. J Neurosci 9:2080-2102.

Kalaska JF, Cohen DAD, Prud'homme M, Hyde ML (1990) Parietal area 5 neuronal activity encodes movement kinematics, not movement dynamics. Exp Brain Res 80:351-364.

Kettner RE, Schwartz AB, Georgopoulos AP (1988) Primate motor cortex and free arm movements to visual targets in three-dimensional space. III. Positional gradients and population coding of movement direction from various movement origins. J Neurosci 8:2938-2947.

Lacquaniti F, Maioli C (1994) Coordinate transformations in the control of cat posture. J Neurophysiol 72:1496-1515.

Masino T, Knudsen EI (1990) Horizontal and vertical components of head movement are controlled by distinct neural circuits in the barn owl. Nature 345:434-437.

Morrison DF (1990) Multivariate statistical methods, pp 312-351. New York: McGraw-Hill.

Mountcastle VB, Lynch JC, Georgopoulos A, Sakata H, Acuna C (1975) Posterior parietal association cortex of the monkey: command functions for operations within extrapersonal space. J Neurophysiol 38:871-908.

Paillard J (1991) Motor and representational framing of space. In. Brain and space (Paillard J, ed), pp 163-182. New York: Oxford UP.

Rosenbaum DA (1980) Human movement initiation: specification of arm, direction, and extent. J Exp Psychol [Gen] 109:444-474.

Sakata H, Takaoka Y, Kawarasaki A, Shibutani H (1973) Somatosensory properties of neurons in the superior parietal cortex (area 5) of the rhesus monkey. Brain Res 64:85-102.

Sakata H, Shibutani H, Kawano K (1980) Spatial properties of visual fixation neurons in posterior parietal association cortex of the monkey. J Neurophysiol 43:1654-1672.

Schwartz AB (1994) Direct cortical representation of drawing. Science 265:540-542.

Schwartz AB, Kettner RE, Georgopoulos AP (1988) Primate motor cortex and free arm movements to visual targets in three-dimensional space. I. Relations between single cell discharge and direction of movement. J Neurosci 8:2913-2927.

Simpson JI, Leonard CS, Sodak RE (1988) The accessory optic system of rabbit. II. Spatial organization of direction selectivity. J Neurophysiol 60:2055-2072.

Soechting JF, Flanders M (1989a) Sensorimotor representations for pointing to targets in three-dimensional space. J Neurophysiol 62:582-594.

Soechting JF, Flanders M (1989b) Errors in pointing are due to approximations in sensorimotor transformations. J Neurophysiol 62:595-608.

Soechting JF, Lacquaniti F, Terzuolo C (1986) Coordination of arm movements in three-dimensional space. Sensorimotor mapping during drawing movement. Neuroscience 17:295-311.

Soechting JF, Helms Tillery SI, Ebner TJ (1992) Discharge of parietal neurons during static postures. II. Relation to postural parameters. Soc Neurosci Abstr 18:503.

Thach WT (1978) Correlation of neural discharge with pattern and force of muscular activity, joint position and direction of intended next movement in motor cortex and cerebellum. J Neurophysiol 41:654-676.